



Waste Heat Utilization at Elkem Ferrosilicon Plant in Iceland

A dissertation by
Heimir Hjartarson

submitted to the Faculty of Industrial Engineering,
Mechanical Engineering and Computer Science
in partial fulfillment of the requirements for
the degree of master of science.

University of Iceland 2009

University of Iceland
Faculty of Industrial Engineering, Mechanical Engineering and Computer Science
VR-II, Hjarðarhaga 2-6, IS-107 Reykjavik, Iceland
Phone +354 525 4700, Fax +354 525 4632
verkognatt@hi.is
www.hi.is

To my beautiful Helena and my son Gunnar Þór.

Abstract

The objective of this study is to look at waste heat utilization at a ferrosilicon plant based at Grundartangi in Iceland with emphasis on electricity production. Other utilization possibilities considered are district heating and steam generation. Currently, Elkem Iceland produces two kinds of products, ferrosilicon and Microsilica®. There is a potential for the third product by utilizing the waste heat. An energy and exergy analysis on furnace 3 is performed based on measurements and data from Elkem Iceland. The production of ferrosilicon involves large exergy destruction, estimated to be 46.5 MW, and the exergetic efficiency of the furnace is about 30 %. The energy analysis shows that much of the energy used in the production of ferrosilicon at Grundartangi goes out to the environment as waste heat. Only 35.6 MW of the 98 MW of the energy supplied to the process are retrieved as chemical energy in the product. Comparison of ORC and steam Rankine cycle configurations were performed and the best configuration gave maximum net power of about 10 MW and 8 MW, respectively. If the waste heat is used in district heating it could supply about 11800 m³/day. Preliminary cost estimate of the capital cost of waste heat recovery cycles was estimated, based on net power output. Estimated capital cost for steam Rankine cycle and ORC is about 2.5 and 4.3 billion ISK, respectively, with about 50 % accuracy.

Útdráttur

Markmið þessa verkefnis er að skoða varmaenduvinnslu hjá Elkem á Grundartanga með áherslu á raforkuframleiðslu en einnig er nýting varmans í hitaveitu og gufu framleiðslu athuguð. Járnblendid framleiðir í dag tvær afurðir, kísiljárn og kísilryk, en einnig er möguleiki á að framleiða þriðju afurðina með því að nýta afgangsvarma. Orku- og exergíugreining er beitt á ofn 3 hjá Elkem og styðjast þær greiningar við mælingar og gögn frá Járnblendinu. Framleiðsla á kísiljárninu hefur með sér í för mikla exergíu eyðingu sem er metin sem 46.5 MW og exergíu nýting ofnsins er áætluð um 30 %. Orkugreiningin leiðir í ljós að mikið af orkunni sem fer í framleiðsu á kísiljárninu skilar sér sem afgangsvarmi út í umhverfið. Af þeim 98 MW af orku sem lagt er inn í framleiðsluferlið skila sér aðeins 35.6 MW sem efnaorka í framleiðsluafurðinni. Gerður er samanburður nokkrum uppsetningum á ORC og gufu Rankine vinnuhringjum gefa bestu uppsetningarnar af hvoru fyrir sig um 10 MW og 8 MW. Ef varminn væri notaður til að framleiða heitt vatn þá myndi fást 11800 m³/dag af 80 °C heitu vatni. Athugun á stofnkostnaði við þær tvær bestu uppsetningar á ORC og gufu Rankine vinnuhring, grundvallað á gefnu afli, gefur að kostnaðurinn er um 2.5 milljarðar við gufu Rankine og 4.3 milljarðar við ORC með 50 % óvissu.

Contents

1	Introduction	1
1.1	Energy intensive industries in Iceland	1
1.2	The Case study - Elkem Iceland	3
1.2.1	History	3
1.2.2	Products	3
1.3	World market and price trends for silicon and ferrosilicon	5
1.4	Structure of the Thesis	6
2	Waste Heat Recovery	7
2.1	Production of Ferrosilicon	7
2.2	Chemistry of the process	10
2.3	Heat Recovery at ferrosilicon plants	11
2.3.1	Elkem Thamshavn	12
2.3.2	Elkem Bjölfefossen	12
2.3.3	Waste gas dynamics	12
2.3.4	Heat Exchangers Design	13

2.4	Working fluid - Rankine vs ORC	14
3	Energy and Exergy Analysis	17
3.1	Chemical model of the furnace	17
3.1.1	The material balance	18
3.1.2	The energy balance	20
3.1.3	Deviation from theoretical process	20
3.2	Energy analysis	21
3.2.1	Input materials	21
3.2.2	Energy from the process	22
3.3	Exergy analysis	24
3.3.1	What is Exergy	24
3.3.2	The furnace	26
4	Utilization	29
4.1	Electricity production	30
4.1.1	Thermodynamics of Rankine cycle	31
4.1.2	Modeling and optimization	34
4.1.3	Steam Rankine working cycle	34
4.1.3.1	Optimization and constraints	35
4.1.3.2	Results for steam Rankine cycle	36
4.1.4	Organic Rankine Cycle	38
4.1.4.1	Fluid selection	40

4.1.4.2	Optimization and constraints	41
4.1.4.3	Results for ORC	42
4.1.5	Steam Rankine vs. Organic Rankine	43
4.2	Other utilizations	45
4.2.1	District heating	46
4.2.2	Steam generation	48
5	Economic analysis	51
5.1	Capital Cost of Power Plants in Iceland	51
5.2	Estimation of Capital Cost for Waste Heat Recovery	53
5.3	Levelized cost of electrical energy	54
5.3.1	Assumptions	55
5.3.2	Sensitivity analysis	56
5.4	More detailed analysis of the ORC	57
5.4.1	Heat exchangers	57
5.4.2	Cost of components	58
6	Conclusion	59
6.1	Further Studies	60
A	Measurements and data analysis	63
A.1	Summary	63
A.2	Off gas	64
A.3	Cooling system	65

A.3.1	The basics	65
A.3.2	Setup	66
A.3.3	Temperature difference	67
A.3.4	Estimated Cooling Load	69
A.4	Directly from furnace	69
A.4.1	Furnace bottom	69
A.4.1.1	Sensors	70
A.4.1.2	The heat flow	72
A.4.2	Furnace sides	74
A.4.2.1	Radiation	75
A.4.2.2	Convection	76
	Bibliography	79

List of Tables

1.1	Statistic about aluminum industry in Iceland [27]	3
3.1	Example of carbon materials on wet basis according to [35], showing the major elements but not complete analysis	21
3.2	Estimated energy delivered to furnace 3 in Elkem Iceland [44]	21
3.3	Summary of heat losses in furnace 3 at Elkem Iceland, \dot{Q}_{OG} is heat loss in Off-Gas, \dot{Q}_{CS} is heat loss through Cooling System, \dot{Q}_{FB} is heat loss from furnace bottom and \dot{Q}_{FS} from furnace sides	23
3.4	Estimated energy from furnace 3 in Elkem Iceland	23
3.5	Estimated exergy delivered to furnace 3 in Elkem Iceland	26
3.6	Estimated exergy from furnace 3 in Elkem Iceland	27
4.1	The key parameter of the optimum solution for the working cycles . .	36
4.2	The state of the working fluid in the optimum configuration T is in $^{\circ}C$ and P is in kPa	37
4.3	Thermodynamic properties of working fluids [32]	40
4.4	The key parameters of the optimum solution for the working cycles . .	43
4.5	The state of the working fluid in the optimum configuration	44

5.1	Estimated capital cost of geothermal power plant projects in Iceland[13, 33]	52
5.2	Typical values for scaling exponent, α [2]	53
5.3	Estimated Capital Investment for waste heat recovery	53
5.4	Rough estimation of the overall heat-transfer coefficient [5, 14, 38] and size of the heat exchangers	57
5.5	Rough estimation of the purchased equipment cost (PEC) [41]	58
A.1	Summary of heat flows	63
A.2	Elkem pitot measurements [44]	64
A.3	Heat load of heat exchanger, Q_{HE} , and total energy in off gas, Q_{OG}	65
A.4	The statistic about the measurements	67
A.5	The statistic for the temperature difference and furnace load	68
A.6	Estimation of the radiation from the furnace	76

List of Figures

1.1	Map of Iceland showing the placement of energy intensive industries (black letters) and projects that are proposed or under construction (red letters)	2
1.2	Reported consumption of FeSi75 by end use in the US in 2006 [31]. . .	4
1.3	World production of silicon and ferrosilicon (left axis) and price trends for FeSi50, FeSi75 and silicon metals (right axis) [31]. Ferrosilicon accounts for about four-fifths of world silicon production	5
2.1	An overview of the quartz to silicon alloy process [17].	8
2.2	Rankine cycle [37]. Main parts are: The boiler with Super Heater (SH), Evaporizer (EV) and Economizer (ECO). Steam Drum (SD). Steam Turbine (ST). Condenser (C). Feed Water Tank (FWT). Water Pump (WP). Pre heating of feed water by Turbine bleed (Tb) is optional	11
2.3	Comparison of T-s diagram for typical wet, dry and isentropic fluids .	15
3.1	The principal process flow in a ferrosilicon production process [35] . .	18
3.2	Chemical model of the furnace	19
3.3	Simplified schematic of furnace 3 at Elkem Iceland and energy losses .	22
3.4	A Sankey diagram of furnace 3 at Elkem Iceland Grundartangi based on the calculated results from the model	24

3.5	A Grassmann diagram of furnace 3 at Elkem Iceland Grundartangi based on the calculated results from the model. The ratio of the streams are based on the input.	27
4.1	A functional analysis of the problem of heat recovery at Grundartangi	29
4.2	A schematic of a simple Rankine working cycle	30
4.3	A schematic of system setup for steam Rankine working cycle for heat recovery at Grundartangi	35
4.4	A TS diagram of the optimum state for the special Steam Rankine cycle. The point for states 3 and 4 are nearly concentric.	36
4.5	The temperature profiles of the Boiler, Cooling System and Condenser for the special steam Rankine cycle	37
4.6	A schematic of an Organic Rankine cycle for heat recovery at Grundartangi, design case one	38
4.7	A schematic of an Organic Rankine cycle for heat recovery at Grundartangi, design case two	39
4.8	A schematic of an Organic Rankine cycle for heat recovery at Grundartangi, design case three	39
4.9	The TS diagram for configuration in Case Two	43
4.10	The temperature profiles of the Boiler, Cooling System and Condenser for the special steam Rankine cycle	44
4.11	The temperature profile in special steam Rankine cycle (left) and ORC Case Two(right).	45
4.12	A schematic of hot water and steam production.	46
4.13	The temperature profile in the heat exchangers to produce hot water .	47
4.14	The mean hot water usage in Akranes for each month in the year 2007 [36]	48
4.15	Mass flow of steam vs. temperature of selected pressures for steam generation	49

5.1	A sensitivity analysis for the levelized cost of electrical energy for steam Rankine cycle. Variables are: specific capital cost, $(\frac{I}{K})_c$, specific O&M cost, $(\frac{O}{K})_O$, discount rate, x , and inflation, y	56
A.1	Simplified schematic of furnace 3 and the heat flow under consideration	64
A.2	The pipe and locations of measurements	66
A.3	Boxplot of the measurement data	68
A.4	Temperature measurements from 12:25 26.11 to 12:25 27.11	69
A.5	The temperature difference over the heat exchanger	70
A.6	The arrangement of temperature, green filled circles, and heat flux sensors, black circles	71
A.7	Contour plot of the furnace bottom temperature at 5:20 27th of November. The green boxes are the positions of the heat flux sensors	72
A.8	Temperature and heat flux for sensor 3.3 on figure A.6	73
A.9	The linear relation for temperature and heat flux, $R^2 = 0.80$	74
A.10	Infrared picture of furnace 3 in Elkem Iceland	75

Acknowledgements

Many people have contributed to this thesis and I want to thank them all deeply. This study was performed under supervision of dr. Guðrún A. Sævarsdóttir and dr. Halldór Pálsson. Guðrún is Assistant Professor at the School science and engineering at the University of Reykjavík and Halldór is Assoc. professor at the Faculty of Industrial-, Mechanical engineering and Computer science. I thank them dearly for their support and assistance.

Elkem Iceland sponsored this study and I owe them and the people there many thanks for their support. Þorsteinn Hannesson at Elkem Iceland receives my greatest gratitude for being very helpful and providing data and information. Also I want to thank Halvard Tveit for his important contribution. Torbjörn Tveitan I want to thank for warm welcome when visiting Elkem Bjölvfossen in Norway and Kjetil Andersen when visiting Elkem Thamshavn.

At NTNU I want to thank Erling Næss and Ladam Yves at SINTEF for their help. At Reykjavík University I want to thank William Harvey for good guidance and help.

Last and not the least I want to thank dearly my family for their moral support.

1 Introduction

The increased awareness of that the world energy resources are limited has been increasing price of prime energy in recent years. Although the current global financial problems has lowered prices again, it is considered only temporary. Increasingly expensive and limited resources for energy call for more sensible use of them. People talk about the need to "conserve" energy, but as we all know quantity of energy is already conserved. The first law of thermodynamics deals with quantity of energy and states that energy cannot be destroyed or created. However in this respect the second law of thermodynamics deals with the quality of energy. Exergy is a concept which captures the essence of the second law of thermodynamics and is used to evaluate the useful part of energy. Exergy is a good tool for analyzing energy systems.

The aim of this study is to look at waste heat utilization at a ferrosilicon plant based at Grundartangi in Iceland. An energy and exergy analysis is performed on one of the furnaces. The utilization of the heat is considered with emphasis on electricity production but district heating and steam generation are also considered.

1.1 Energy intensive industries in Iceland

In Iceland there is not long history for energy intensive industries. They have been established in the recent decades, coincident with the harnessing of Iceland's hydro and geothermal power. The two major kinds of energy intensive industries in Iceland are aluminum smelting and ferrosilicon production. Figure 1.2 shows a map of Iceland and the placement of the current aluminum smelters and proposed aluminum smelters. The most recent smelter operating is based in Reyðarfjörður east in Iceland and one smelter project is under construction in Helguvík, with environmental oper-

ating permit (EOP) for 250 000 tons of aluminum per year. Another smelter project is proposed at Bakki in north of Iceland, also with EOP for 250 000 tons per year.

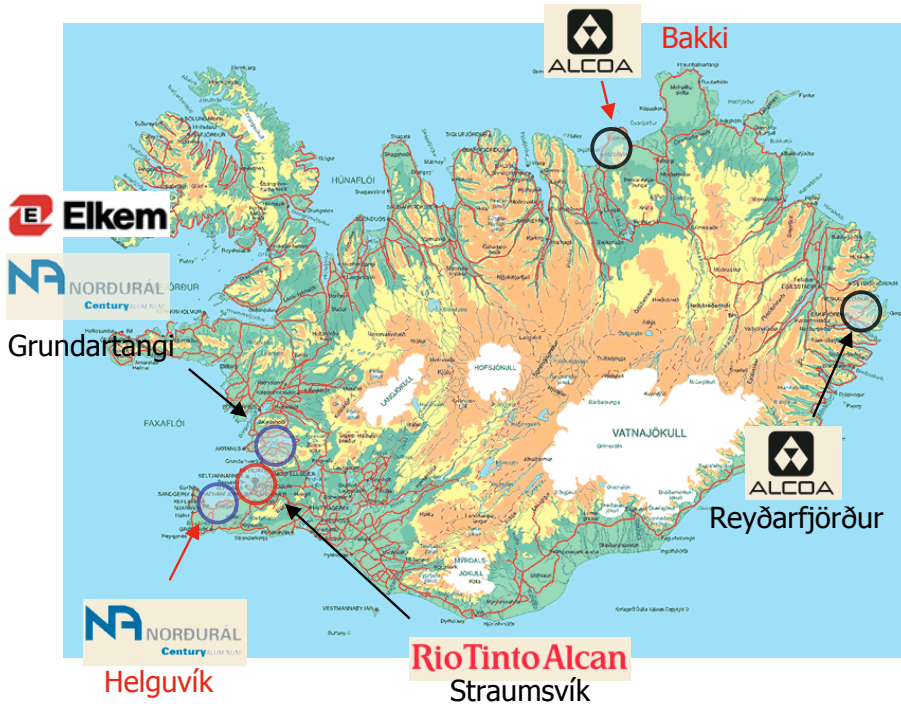


Figure 1.1: Map of Iceland showing the placement of energy intensive industries (black letters) and projects that are proposed or under construction (red letters)

The aluminum industry is the largest user of electricity in Iceland and it alone uses nearly 70 % of all produced electricity in Iceland while the ferrosilicon plant at Grun-dartangi uses about 8.6 % [27]¹. In table 1.1 is an overview of the current operating aluminum plants in Iceland and their statistic.

¹based on figures for the year 2007

	EOP ²	Power used	Production in 2007
Alcan Straumsvík	460 000 ton	335 MW	183 000 ton
Century Al. Grundartangi	300 000 ton	440 MW	240 000 ton
Alcoa Reyðafjörður	346 000 ton	560 MW	35 490 ton ³
Total	1 106 000 ton	1 335 MW	458 490 ton

Table 1.1: Statistic about aluminum industry in Iceland [27]

1.2 The Case study - Elkem Iceland

1.2.1 History

Elkem Iceland is located at Grundartangi in Hvalfjörður as illustrated in figure 1.1. It was founded by the Icelandic government in cooperation with the American corporation Union Carbide on April 28, 1975, and was then called Icelandic Alloys Ltd. A year later the Union Carbide withdrew from the project and was replaced by a Norwegian company named Elkem. The first years of the plant operation were difficult and in 1984 the company was restructured and a new partner, Sumitomo Corporation, became a shareholder. Elkem took over the company in 2003 and is today part of Orkla ASA [9, 17].

Elkem Iceland operates three furnaces for their ferrosilicon production. The first two were commissioned in 1979 and 1980 and are 36 MW. The third one was commissioned in 1999 and is 47MW.

1.2.2 Products

The main product of Elkem Iceland is ferrosilicon, which is denoted as FeSi75 and is 25 % iron and 75 % silicon by weight. Silicon is denoted by numbers and thus for FeSi45 is 55 % iron and 45 % silicon by weight. A byproduct is condensed silica fume (CSF) or Microsilica® which is amorphous SiO_2 and has specific surface area around 20 m^2/g . The third product of the process could be recoverable heat energy but current configuration of the plant does not utilize that [35].

Ferrosilicon is produced in an electric arc furnace with high temperatures, about 2000 °C. The recipe to produce one ton of FeSi75 is as following: About 2 tons of quartz,

²EOP stands for Environmental Operating Permit

³Production started in spring 2007

about one ton of coal and coke, $\frac{1}{3}$ ton iron in some form (e.g. mill scales), 50 kg of electrode material and about 9 MWh of electricity. Also limestone and wood chips are added but wood chips are the only locally available product, beside the electricity.

The yearly production at Grundartangi is about 120 000 tons of FeSi75 and is that about 1.3 % of the world silicon metal production, estimated by the Mineral Resource Program at the U.S. Geological Survey (USGS) [31]. The largest application of ferrosilicon is in steel and cast iron production where the task of the ferrosilicon is to bind and remove oxygen and oxides. As illustrated in figure 1.2 less than 1 % of FeSi75 consumption in the US goes to other application than steel and cast iron [31]. The USGS defines FeSi75 as ferrosilicon with silicon content in ranges between 56% to 95%.

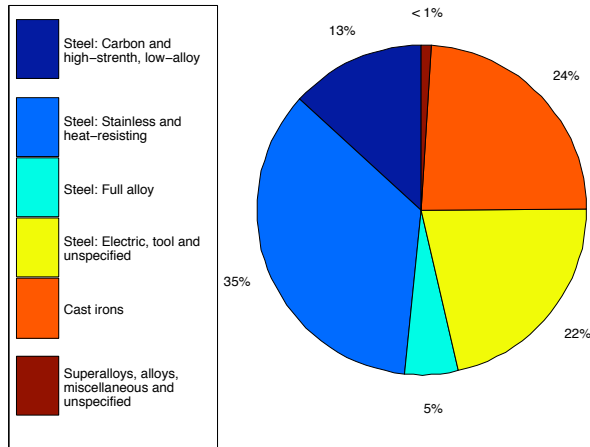


Figure 1.2: Reported consumption of FeSi75 by end use in the US in 2006 [31].

Elkem Iceland recently started producing a more specialized product, FSM (Ferro, Silicon, Magnesium), in furnace one. This product is used in foundries and is priced higher. The CSF from Grundartangi is used as a additive in cement in Iceland and elsewhere [17, 35].

1.3 World market and price trends for silicon and ferrosilicon

The prices and production of silicon and ferrosilicon have been going up in recent years as illustrated in figure 1.3. However, because of global financial problems that began in third quarter of 2008, the demand has been decreasing and prices for silicon and ferrosilicon have declined. This recent development is not seen in figure 1.3.

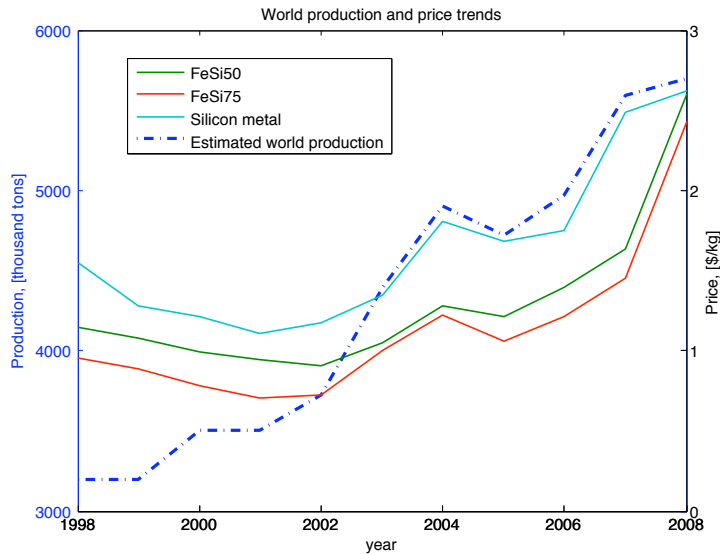


Figure 1.3: World production of silicon and ferrosilicon (left axis) and price trends for FeSi50, FeSi75 and silicon metals (right axis) [31]. Ferrosilicon accounts for about four-fifths of world silicon production

Figure 1.3 also illustrates the estimated world production of silicon material [31] and ferrosilicon accounts for about four-fifths of the total. It is remarkable that the production capacity has nearly doubled in 10 years time. The leading producer of silicon materials in 2008 in descending order are China with 60 % of world production, Russia with 11 %, Norway with 6 % and Brazil with 5 %. It is noticeable that China is by far the leading producer of silicon materials in 2008, both in ferrosilicon and silicon metal, 2,700,000 and 560,000 tons, respectively.

1.4 Structure of the Thesis

The structure of the thesis is as follows:

Chapter 2 describes the ferrosilicon process and the plant and also includes discussion on how waste heat is recovered in similar plants in Norway. The chapter also lists some pros and cons of organic working fluids for heat recovery.

Chapter 3 contains energy and exergy analysis of furnace 3 which is part based on measurements and data analysis that is explained in detail in [appendix A](#).

In chapter 4 utilization of the waste heat is considered, focusing on electric production by steam Rankine and Organic Rankine cycle. Though the focus is on electricity production, some discussion is included on steam generation for industrial use and hot water production for district heating.

In chapter 5 the capital cost of heat recovery plant is estimated and the levelized cost of the electric energy production evaluated. The economic analysis will approach the problem from the top down and is rough estimate but gives an idea of the cost.

Finally, Chapter 6 includes conclusion and suggestions for future work.

2 Waste Heat Recovery

Efficient use of all energy resources is becoming more important with regard to both sociological and economical grounds. Waste heat sources are plentiful in industrial plants and are often not treated with enough respect as useful energy. Typical waste heat sources are:

- hot gases from blast furnaces in steel industry
- exhaust gases of gas turbines and diesel engines
- hot gases from kilns in ceramic industry
- thermo oil or other hot liquid used to cool kilns in buildings material industry
- hot liquids in paper and pulp industry

More unconventional waste heat sources are low temperature e.g. as in the aluminum industry where the temperatures are below 200 °C. The basic idea, according to Larjola [23], is that thermal energy that cannot be used efficiently in a plant process or in a district heating system, may be called waste heat, and will have value only if it can be converted to electric power [23]. To be able to recover heat from a process it is essential to know the process and therefore the following chapter describes ferrosilicon process.

2.1 Production of Ferrosilicon

A ferrosilicon plant can be divided into four main groups:

- the handling of raw material
- the furnace including the electrical supply
- the system for cleaning of waste gas including energy recovery
- the post-taphole treatment of metal

The handling of raw material includes transport, storage, weighing and mixing. A schematic picture of the overall process is in figure 2.1.



Figure 2.1: An overview of the quartz to silicon alloy process [17].

At Grundartangi the raw materials are imported by ships, except the wood chips which are provided locally. The raw materials are stored outdoors or in a shelter. The material is then transported to a conveyor belt which transfers the raw material to "day bins", that are smaller storage. A conveyor system takes raw material from the "day bins" and weighs it and mixes in right portions and brings them to the furnace.

A furnace includes

- Electricity supply consisting of electric grid, transformers, bus bars and the electrodes

- Equipment for adding raw material
- A furnace shaft consisting of shell and a lining that can resist extremely high temperatures and attack by chemicals
- Equipment for tapping the alloy from the lower part of the furnace body

The core of the plant is the furnace. A typical furnace is about 10 m in diameter and consists of a hood and the body. The hood is the upper part of the furnace and is water cooled. The body consist of an outer steel shell and an inner lining that can resist the extreme temperature and attack from chemicals. Furnace one and two at Grundartangi were designed as semi-closed but the newest furnace was designed as split-body furnace with the possibility of closing it later. The benefits of closed furnace are lower gas volume and the option of recovering CO and H₂. According to [35] average composition of CO and H₂ in the off gas of a closed FeSi75 furnace are about 70% and 20%, respectively. This could be used for some chemical process like producing methanol or diesel oil with Fisher-Tropsch method. The disadvantage is that the off-gas becomes dirtier and contains tar, which burns with excess air in the semi-closed furnace. The closed furnace set up has been more successful for lower grade of silicon like FeSi45.

Three electrodes are submerged into the furnace pot and the pot is filled with charge material. Through the electrodes a three-phase current is passed through the charge material. At Grundartangi the electrodes used are a "Söderberg" type which are consumed by the process. The heat from the furnace and the electrical resistance bake them continuously from carbon paste to a solid electrode in steel casing over the furnace. The material is fed to the furnace by automatic leading system. When the material is fed to the furnace the charge is stocked. The furnaces need to be stoked regularly to keep the melt homogenous and prevent SiO_(g) from escaping through it.

The system for cleaning the waste gas at Grundartangi does not include energy recovery. But the waste gas is cooled down with heat exchangers which exchange heat with the environment. In the waste gas is condense silica fume (CSF) which is a valuable product. Therefor the waste gas is led through filters and CSF is collected into bags.

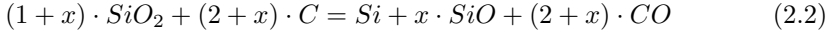
It is important to tap the metal at regular interval, otherwise the metal that could be collected goes to the filter as CSF. The metal is at 1600 °C when tapped into a crucible 5 tons at a time. There are different ways of handling the metal after tapping. At Grundartangi the FeSi75 metal is cast in iron moulds and then rapidly cooled down with water shower, which is important to get small grain size. The metal blocks are then crushed to sizes suitable for different customers.

2.2 Chemistry of the process

The chemistry of ferrosilicon process is quite complicated. It involves a lot of physical and chemical relations but the overall chemical reaction can be written as:

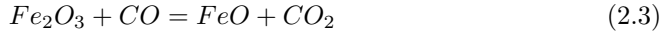


Iron is not included in this equation and to be short it serves as a catalyst for the overall process and the production becomes easier with increasing iron content of final product [35, 43]. The production of pure silicon and ferrosilicon is very similar. A more complex description of the reaction is:



where x is defined as $R = \frac{1}{1+x}$ or $x = \frac{1-R}{R}$, where R defines the silicon yield. The silicon yield is preferred high because the FeSi75 metal is more valuable than the CSF. Compared to pure silicon production, the addition of iron as in FeSi75 production, increase silicon yield [35].

Reduction of hematite, Fe_2O_3 , can be either done by CO and CH_4 or CO and C, which is assumed here and in the model introduced later. The reduction is done in two steps. First the hematite is reduced to FeO by mean of a reaction with CO [25, 35]:



Then FeO reacts with carbon in following reaction:



For other ratios of ferrosilicon the reduction can be totally with C or a mix of these two cases with CH_4 and CO [25].

2.3 Heat Recovery at ferrosilicon plants

The heat recovery in the ferro alloy industry was initiated by the need to cool the off gas before it enters the filters. According to [37] of 16 ferro alloy plants in Norway only 3 recover heat to produce electricity and 5 to produce thermal energy. Two of those that produce electricity, Thamshavn and Bjölvfossen will be looked at closer.

The technology used to recover this heat and convert it to electricity is the steam Rankine cycle. A schematic in figure 2.2 illustrates this idea: The systems in Bjölvfossen and Thamshavn are based on this principle. The heat from the off gas is recovered by three steps: economizer (ECO) heats the water up to the saturated vapor line that subsequently passes to the steam drum SD. Then the water vaporizes in the evaporizer (EV) and is then superheated as steam in the superheater (SH) before it enters the steam turbine (St). Because this is a steam Rankine cycle, superheating is necessary to avoid too much condensation in the turbine, if the enthalpy drop over the turbine is to be large. The steam from the turbine is then condensed in a condenser (C). Optional is to bleed steam from the turbine to heat up the water from the condenser before it enters the economizer again.

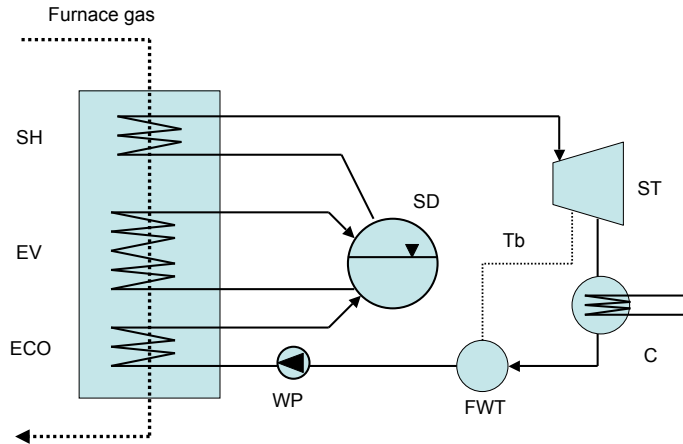


Figure 2.2: Rankine cycle [37]. Main parts are: The boiler with Super Heater (SH), Evaporizer (EV) and Economizer (ECO). Steam Drum (SD). Steam Turbine (ST). Condenser (C). Feed Water Tank (FWT). Water Pump (WP). Pre heating of feed water by Turbine bleed (Tb) is optional

2.3.1 Elkem Thamshavn

Elkem Thamshavn operates two semi-closed silicon furnaces, 26 MW and 43 MW, that were converted from ferrosilicon some years ago. The off gas from the furnaces is taken through one waste heat boiler which was designed as fluid-bed boiler. Sand particles were supposed to clean the boiler and keep the heat transfer high but this method was abandoned due to erosion and the boiler was redesigned for shot-cleaning which is continuous because of intensive fouling [37].

The configuration of the boiler makes the off gas flow upward and the steel clips are dropped down the boiler from above. There is problem with this configuration, first because the furnace gas tends to blow the steel clips up ward, therefore reducing their effect and secondly the scaling is collected on the piping lower surface out of the reach of the steel clips.

The off gas from both furnaces, which is about 700 °C, is led through one common heat exchanger consisting of 4 economizers, 2 evaporators and 2 superheaters [37]. The steam from the boiler is approximately 460 °C and 50 bar. The turbine, which is a multi-stage reaction turbine produces about 17 MW and 105 GWh per year. The condenser utilizes sea water which is about 4 to 15 °C.

2.3.2 Elkem Bjölvefossen

Elkem Bjölvefossen produces FeSi51 and operates two semi-closed furnaces, 17 MW and 24 MW, built 1981 and 1976, respectively. Production of FeSi51 is easier than Si metal. The boilers were designed from the beginning for shot cleaning and they are two, one for each furnace. This boiler configuration is preferred [39]. The furnace gas stream about 750 °C and is in the same direction as the shot-cleaning. The steam from the boiler is about 420 °C and 28 bar and the turbine produces about 6.5 MW or 52 GWh per year. The steel ball cleaning is done when the pressure drop over the heat exchanger is over some limit and that is about once an hour [40].

2.3.3 Waste gas dynamics

New and stricter environmental regulations have forced industries to get a more fundamental understanding of their process to understand better of what is going on. According to [19] large variations are in the composition and temperature of waste gas from ferrosilicon furnace. The variations are found during normal furnace operation such as stoking and charging.

Batch-wise operation gives more fluctuations in waste gas composition and temperature, while continuous operation is more stable and gives higher average gas temperature that will increase heat recovery and make it more valuable product. Other factors also important are selection of raw material and regular stocking [19].

The temperature of the gas exiting a furnace can vary a lot as seen in the ferrosilicon plant in Thamshavn[19]. There the average temperature of the off gas exiting a 42 MW furnace was 725.5 °C with a minimum of about 330 °C and maximum about 1400 °C, but those peaks and lows were only for short time. The range in temperature for batch-wise furnace operation is therefore about $r = 1100$ °C. These fluctuations are not good for heat recovery. With continuous feeding the average temperature was about 750 °C with a minimum of 670 and a maximum of 900 °C which give the range about $r = 230$. From this information it can be concluded that good furnace operation is important part of heat recovery.

Limitations

A limiting factor of heat recovery is the fact that the furnace gas cannot be cooled down below certain point before entering the filters. This point depends on the off gas composition and varies from 150 - 220 °C [37, 44]. If lower temperatures are found it may cause severe corrosion in the gas filter and colder parts of the boiler. This is due to condensation of sulphuric acid. In practice this corrosion hazard is the reason that when a furnace is shut down temporarily it is necessary to keep the heat recovery system above this certain temperature to avoid condensation [40].

2.3.4 Heat Exchangers Design

The boilers in Thamshavn and Bjölvefossen are designed as vertical crossflow heat exchangers where the furnace gas is drawn over bank of tubes filled with water [39, 40]. This kind of boiler configuration is called watertube and is the most common in the process of recovering heat from flue gases [5]. The ferrosilicon plant in Salten Norway has this though the other way around. There the furnace gas is inside the tubes and the water on the outside. This configuration is called firetube and does not allow as high pressures of the steam and is therefore restricting. The maximum pressure for firetube boiler design is about 1.7 MPa were as the operational pressure before the turbine in Bjölvefossen is about 2.8 MPa.

As mentioned here there are large temperature swings in the flue gas and this is important for the boiler design. A boiler can be designed as free circulation or with forced circulation with pumps. The pumps are constant flow and do not cope well

with large variations while free circulation solves this problem because of no flow restriction. This is important in the earlier stages of the boiler where the gas is the hottest, the superheater and the cooling system of the hut and off gas channels from the furnace.

Fouling consist of deposition of material on heat transfer surface. The silica is tricky dust. The shear forces in the flow are not able to stop deposition of material on the tubes and therefore external cleaning is needed. The small particles in the off gas stick to the surface of tubes. As mentioned earlier the waste gas composition varies a lot and when stoking is done in the furnace, larger particles are released which sandblast the tubes in the boiler [26]. Also according to [19] part of the clogging problem in boilers can be solved with CO combustion. If water gets into the dust it get very sticky and the scaling becomes very though.

At Thamshavn the boiler system is about 30 years old and needs to be replaced. The new design will be based on the Bjölvefossen idea. As mentioned, there will be one boiler for each furnace which is preferred over one common boiler for all the furnaces. In the boiler design good spacing between components for inspection and cleaning is necessary [40].

2.4 Working fluid - Rankine vs ORC

The typical working fluid for waste heat recovery in silicon and ferrosilicon production is steam [37]. But steam is not as flexible as organic fluid when it comes to heat exchange from the furnace gas. Organic Rankine cycle (ORC) is a cycle, where the working fluid consist of hydrocarbons instead of water. According to [37], it is advised to avoid technologically complicated solutions in the process of heat recovery in ferro alloy industries but the complexity level of he ORC is comparable to the steam Rankine cycle.

Waste heat utilization can be divided into three types based on the temperature of the waste heat stream [23]. High temperature is about 500 °C and over and often in such cases the water is the best working fluid. Low temperature is defined as below 200 °C and ORC, Kalina and other methods have more advantage over the steam. In the medium range, between 200 and 500 °C both steam and organic working fluids have their advantage. The advantage of organic fluid is that its specific vaporization heat is much lower than that of water and therefore the temperature in the organic working fluid "follows" better that of the heat source fluid to be cooled, reducing entropy generation [23].

Working fluids for Rankine cycle can be categorized into three different groups based

on the types of slope according to the temperature-entropy (T-s) diagram on their saturation vapor curves [15]: .

1. Dry fluids that have positive slopes, generally of high molecular number, e.g. R113, Benzene and Toluene
2. Wet fluids that have negative slope, generally of low molecular number, e.g. water
3. Isentropic fluids that have nearly vertical saturated vapor curves, e.g. R11 and R12

Figure 2.3 illustrates this by comparing the T-s diagram of water and toluene and R113 and R11.

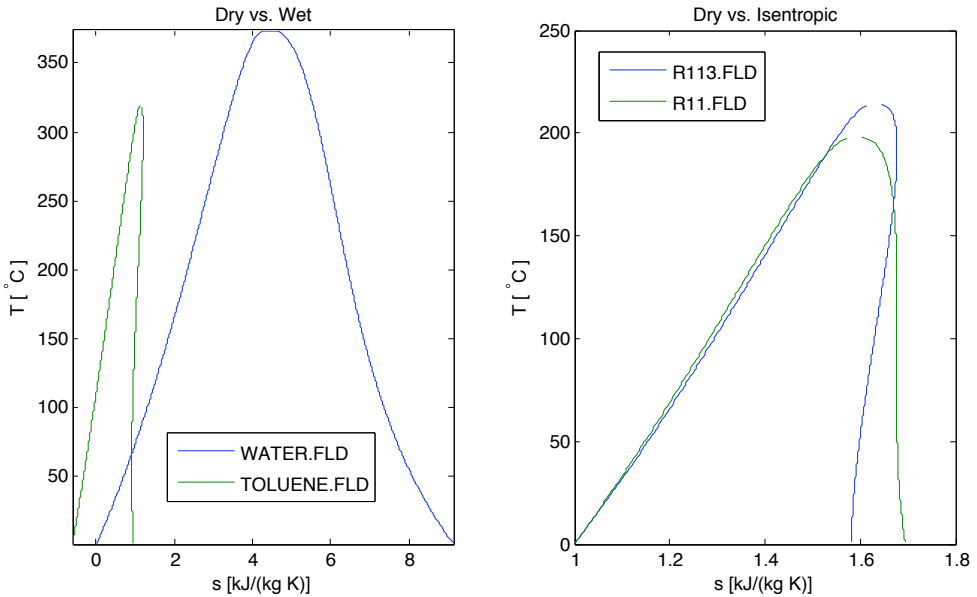


Figure 2.3: Comparison of T-s diagram for typical wet, dry and isentropic fluids

The dry and isentropic fluids have one big advantage, which is that when they go through the turbine and have a large enthalpy drop, one has not to worry about the quality of the fluid that can damage the turbine as the saturation curve has positive slopes, on both the liquid and vapor side. In most cases a single stage turbine may be used instead of multi-stage turbine, as required for steam [23]. The reason for

this difference is related to the presence of hydrogen bond in those molecules, such as water, ammonia, and ethanol which results in wet fluid characteristics. [24].

The possible working fluids for use in Rankine cycle are many and the choice comes down to good thermodynamic properties. When an organic working fluid is being considered the following has to be kept in mind: toxicity, explosion- and flammability characteristic, material compatibility and fluid stability limits [15].

3 Energy and Exergy Analysis

In this analysis the focus will be on furnace 3 at Elkem Iceland. Before starting analyzing the furnace, a model is made to evaluate all the different chemical, mass and energy relations. From these relations and actual input data from Elkem Iceland, the energy and exergy analysis is made.

3.1 Chemical model of the furnace

Here a chemical model will be developed with the focus on the energy and material balance for the system. The assumptions for the model are:

- Furnace operation is assumed to be at steady state
- Air is considered to be composed of 20% O_2 and 80 % N_2
- Chemical reactions are considered to complete fully
- The changes of potential and kinetic energy of materials going into the furnace and coming out of the furnace are neglected
- Gases are assumed as ideal

The production of ferrosilicon is complicated process and to get an overview a simplification is needed. According to [35] the ferrosilicon process flow can be divided into four main parts:

1. Upper part of the furnace - Heat exchange between the electrode, cold raw material and the furnace gas.
2. Submerged arc furnace - Reduction of iron oxide and quartz takes place
3. Product treatment - Solidification and cooling of the metal
4. Gas treatment - the combustion of gas from the furnace by adding air

This segmentation of the furnace is illustrated graphically in figure 3.1 with the assumed temperatures of the process streams.

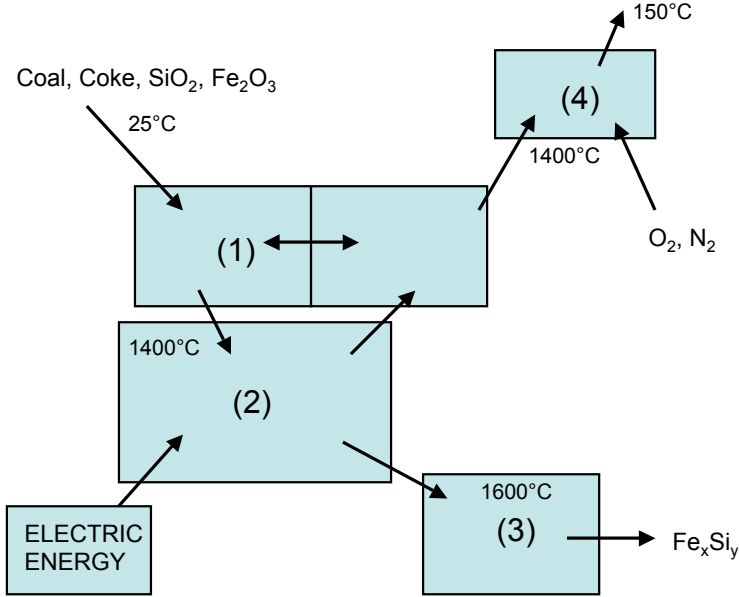
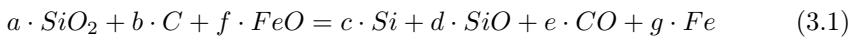


Figure 3.1: The principal process flow in a ferrosilicon production process [35]

3.1.1 The material balance

The core reaction of the model is in the *submerged arc furnace* part and is that the reduction of the quartz and iron oxide with carbon and electricity :



and the coefficient can be found with mass balance and are based on the silicon yield, R . The gas products of the chemical reaction are considered to be at 1400 °C and the metal products are at 1600 °C. The gases rise up to the *gas treatment* part and are mixed with excess air and burned. Not all of the gases are burned, part of the CO is used to reduce the hematite, Fe_2O_3 , to iron oxide, FeO , as presented in:

$$\frac{f}{2} \cdot Fe_2O_3 + \frac{f}{2} \cdot CO = f \cdot FeO + \frac{f}{2} \cdot CO_2 \quad (3.2)$$

with the same coefficient as in equation 3.1. From the *submerged arc furnace* the metal goes into *product treatment*, at 1600 °C, where it solidifies and cools down. After the *gas treatment* the gases, from equation 3.1 and 3.2, leave the furnace at 450 °C. The chemical model is illustrated graphically in figure 3.2.

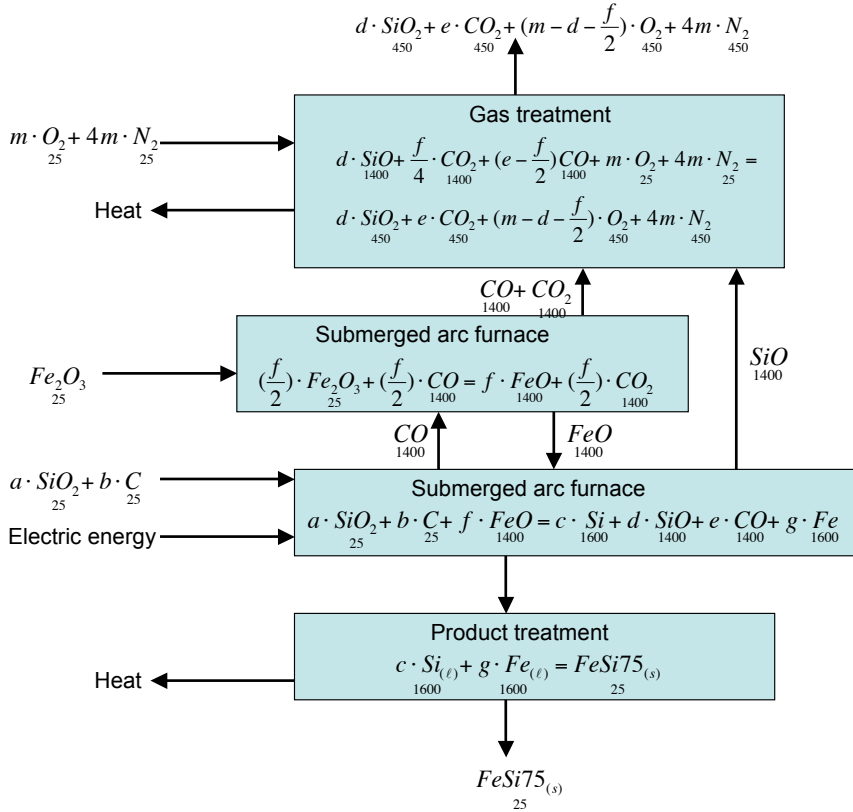


Figure 3.2: Chemical model of the furnace

3.1.2 The energy balance

From the model in figure 3.2 the energy in the chemical reactions is calculated using thermochemical data from reference [7]. The energy balance for reactions in steady-flow system is defined as [6]:

$$\dot{Q}_{in} + \dot{W}_{in} + \sum \dot{n}_r \cdot (\bar{h}_f^o + \bar{h} - \bar{h}^o) = \dot{Q}_{out} + \dot{W}_{out} + \sum \dot{n}_p \cdot (\bar{h}_f^o + \bar{h} - \bar{h}^o) \quad (3.3)$$

where \dot{n}_r and \dot{n}_p represent the molar flow rate of the product p and reactant r, respectively. \bar{h}_f^o is enthalpy of formation and $\bar{h} - \bar{h}^o$ is the difference of sensible enthalpy at the given state and the sensible enthalpy at the reference state. With mass balance and energy balance the energy flows in the process can be calculated.

3.1.3 Deviation from theoretical process

The ideal process described in the preceding chapters and the real industrial process are not the same. The main difference between the industrial process and the theoretical are: 1) energy losses from the process, 2) the use of non-pure carbon 3) carbon losses to the off-gas system and 4) other minor deviations from an ideal process [35].

The energy losses show up as heat in the cooling water, heat in the furnace gas and heat directly from the furnace. There is also loss of electric energy because of resistance in the electrode. The electric energy is of high current and low voltage and therefore resistance plays a big part. Energy losses from the electrode can be found as heat in the furnace gas and the cooling system.

As illustrated in figure 3.2, the theoretical process uses pure carbon but a real process needs to get its carbon from carbon materials, like coal, coke, charcoal and wood chips. These materials include moisture, volatiles, ash and other elements. Typical analysis of these carbon materials are given in table 3.1.

Some of the carbon used in the ferrosilicon process is lost to the furnace gas by draft, where it burns. The draft is because of the need to control the temperature in the furnace gas and ensure complete capture of the flue gases in the *gas treatment* part of the furnace. This carbon loss is typically around 5 % but varies from furnace to furnace. Other minor deviations are e.g. minor elements, like aluminum oxides, that are recovered in the product and "steal" energy from the process as they are reduced with the ferrosilicon [35].

Type	Fixed Carbon %	Volatile %	Moisture %	Ash %
Coke	75	4	16	4
Coal	51	35	12	2
Charcoal	46	8	39	6
Wood Chips	12	35	52	1

Table 3.1: Example of carbon materials on wet basis according to [35], showing the major elements but not complete analysis

3.2 Energy analysis

The energy analysis is based on the chemical model introduced in chapter 3.1 and actual input data from Elkem Iceland [44]. The ferrosilicon process is a batch process and the materials have some lag time in the furnace. One of the assumptions is that the furnace is modeled as continuous process and therefore the mean input data over 7 days was acquired to minimize error.

3.2.1 Input materials

The carbon material fed to furnace 3 in Grundartangi are only Coke and Coal. An actual chemical analysis of the carbon materials [44] was used to estimate the amount of carbon, volatiles and moisture supplied to the furnace. Other minor elements were ignored. The volatiles in the carbon materials are assumed to be methane, CH_4 , and burn in the *gas treatment* part of the furnace. They do not take part in the reduction process [25] but add energy to the process. The quartz was also considered to be pure and all the iron to the process was assumed to be hematite. From the input data from Elkem Iceland [44] the energy of input materials and electricity is estimated and presented in table 3.2. The mean silicon yield for the time period was $R = 89 \%$.

Energy type	Energy into the process	Part
Electric Energy	39.7 MW	40 %
Chemical Energy Fix Carbon	33.1 MW	34 %
Chemical Energy volatiles	25.2 MW	26 %
Total	98 MW	100 %

Table 3.2: Estimated energy delivered to furnace 3 in Elkem Iceland [44]

The calculated energy use from the theoretical model to reduce the quartz was 34.2

MW while the actual measured power use at Elkem was 39.7 MW. This is about 16 % difference and is in good relation with the literature. According to [35] the mean difference in the theoretical energy usage and the measured energy usage of real furnace is 16 %. Also according to the theoretical model the carbon needed for the process is 8 % less than used in the real furnace.

3.2.2 Energy from the process

The main energy losses are heat in the cooling system, losses directly from the furnace and heat lost by the furnace gas. This is illustrated in a simplified schematic of the furnace in figure 3.3, where \dot{Q}_{OG} is heat losses in Off-Gas, \dot{Q}_{CS} is heat loss through the Cooling System, \dot{Q}_{FB} is heat lost from Furnace Bottom and \dot{Q}_{FS} is heat lost from Furnace Sides.

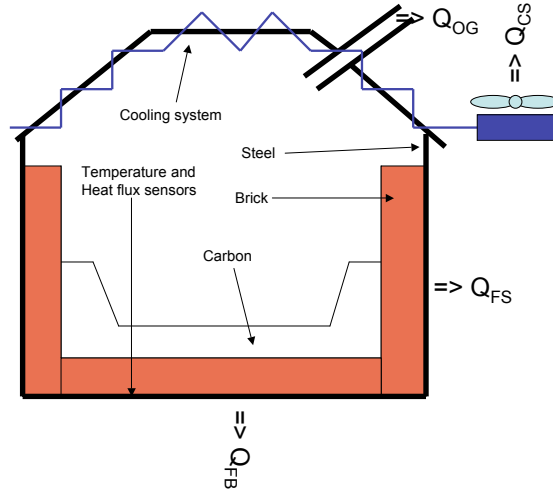


Figure 3.3: Simplified schematic of furnace 3 at Elkem Iceland and energy losses

The energy losses for furnace 3 have been estimated from measurements and data analysis at Elkem Iceland and the methods and the outcome is presented in appendix A. The results are summarized in table 3.3.

In the energy balance of the model, an account is taken for the energy losses directly from the furnace, \dot{Q}_{FB} and \dot{Q}_{FS} , and the losses in the cooling system. The rest of the heat from the chemical reactions in the process is assumed to be taken out by heating of excess air in the *gas treatment*. Therefore any error in the measurements becomes

	MW	%
\dot{Q}_{OG}	43.5 ± 4	76.3
\dot{Q}_{CS}	12.7 ± 0.9	22.3
\dot{Q}_{FB}	0.45 ± 0.2	0.8
\dot{Q}_{FS}	0.33 ± 0.13	0.6
Total	57 ± 5.2	100

Table 3.3: Summary of heat losses in furnace 3 at Elkem Iceland, \dot{Q}_{OG} is heat loss in Off-Gas, \dot{Q}_{CS} is heat loss through Cooling System, \dot{Q}_{FB} is heat loss from furnace bottom and \dot{Q}_{FS} from furnace sides

as error in the furnace gas. The model results for the estimated energy output are presented in table 3.4.

Energy type	Energy from the process	Part
Chemical energy product	35.6 MW	36 %
Heat in product	3.5 MW	4 %
Energy in off-gas	45.5 MW	46 %
Cooling System	12.7 MW	13 %
Directly from furnace	0.8 MW	1 %
Total	98 MW	100 %

Table 3.4: Estimated energy from furnace 3 in Elkem Iceland

According to the results it can be seen that most of the heat is contained in the furnace gas. The model estimate is 5 % higher than the estimated heat in the off-gas from the measurements in appendix A. This is small error and the reason for this difference could be that there is not taken account for reduction of minor elements and that the heat loss directly from the furnace is underestimated.

More important though is the fact that the measurements were performed at different times and at different loads as of the mean furnace load in the model. The mean load for the input data for the model was 39.7 MW while when the off gas was measured the mean load was 43 MW. Also the heat in the cooling system was measured when the load was 45 MW and therefore in the energy balance of the model, the estimated heat losses from these parts are overestimated. This is beneficial for the result as the error of the model cancels out the error cause by different loads in the measurements. A Sankey diagram based on the results from the model is presented in figure 3.4.

As seen there of the total 98 MW of energy supplied to the furnace only 35.6 MW is

returned as chemical energy in the product. The rest of the energy goes off as waste heat and a good portion of that heat could be recovered by simple means.

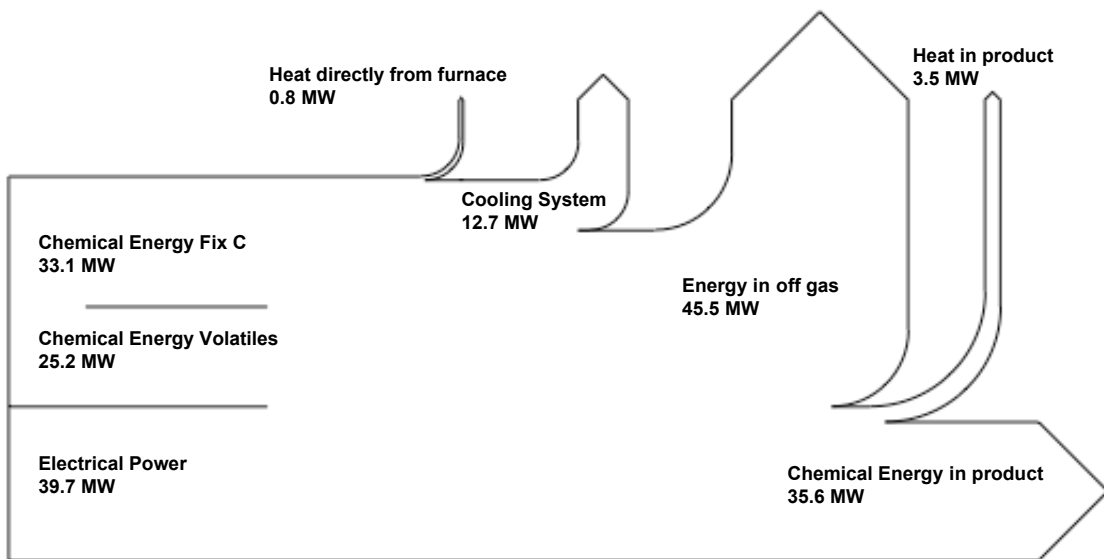


Figure 3.4: A Sankey diagram of furnace 3 at Elkem Iceland Grundartangi based on the calculated results from the model

3.3 Exergy analysis

3.3.1 What is Exergy

Exergy is a measure of quality of energy. As we know it is not possible to destroy energy but it is possible to waste exergy. But in order to define exergy, a reference state is needed, the so called dead state. A system is said to be in dead state when it is thermodynamic equilibrium with the environment. In this analysis the dead state is defined the same as the standard state, that is:

$$\begin{aligned} t_0 &= 25 \text{ }^{\circ}\text{C} \\ p_0 &= 100 \text{ kPa} \end{aligned}$$

The choice of this dead state temperature is because of the standard dead states is commonly defined as this. This is valid especially for chemical exergy and the error caused by this assumption is not that much when dealing with solids and gases [21]. Exergy can be divided into distinct components, that is:

$$\dot{E} = \dot{E}_k + \dot{E}_p + \dot{E}_{ph} + \dot{E}_0 \quad (3.4)$$

where \dot{E}_k is kinetic exergy, \dot{E}_p is potential exergy, \dot{E}_{ph} is physical exergy and \dot{E}_0 is chemical exergy.

Kinetic and potential exergy

Kinetic and potential exergy are defined as following:

$$\dot{E}_k = \frac{1}{2} \cdot V^2 \quad (3.5)$$

$$\dot{E}_p = g \cdot z \quad (3.6)$$

where V , [m/s], is velocity, g , [m²/s], is gravity and z , [m], is elevation.

Physical exergy

Physical exergy associated with stream of matter is defined as:

$$\dot{E}_{ph} = (h - h_0) - T_0 \cdot (s - s_0) \quad (3.7)$$

where h and s are enthalpy and entropy of the stream and h_0 , s_0 and T_0 are enthalpy, entropy and temperature of the dead state.

Chemical exergy

Chemical exergy can be defined as equal to the minimum work that has to be done to the environment to synthesis the chemicals that are considered, only by using heat

transfer and exchanges of substances that are found in the environment. For solid substances at atmospheric pressure it is enough to use standard chemical exergy, $\tilde{\epsilon}^0$ [kJ/kmol], to calculate the chemical exergy. For a gas mixture at atmospheric pressure it is also necessary to account for different composition from the environment and the following equation is used:

$$\dot{E}_0 = \sum x_i \cdot \tilde{\epsilon}^0 + \tilde{R} \cdot T_0 \cdot \sum x_i \cdot \ln x_i \quad (3.8)$$

where x_i is the molar portion of gas mixture component i and \tilde{R} is the universal gas constant [2].

3.3.2 The furnace

For the exergy analysis of the furnace the same assumptions are made in the chemical model as in the energy analysis. One of the assumptions states that potential and kinetic energy are neglected and the same will apply for the exergy analysis. Standard chemical exergy of the raw materials was used according to reference [21].

The exergy equations were employed on the model and the exergy of the material streams and electricity entering the furnace and material streams exiting were evaluated. The results for the exergy into the furnace are presented in table 3.5. The air is considered to have zero exergy as it is part of the environment.

Exergy type	\dot{E}_{ph}	\dot{E}_0	$\dot{E}_0 + \dot{E}_0$	Part
Electric Energy	39.7 MW	0	39.7 MW	40 %
Raw material	0	58.4 MW	58.4 MW	60 %
Air	0	0	0	0

Table 3.5: Estimated exergy delivered to furnace 3 in Elkem Iceland

The exergy of the streams exiting the furnace are presented in table 3.6. It can be clearly seen that the quality of the energy from the cooling system is very low. The exergy is only about 1 MW and is 2 % of the output while compared to 13 MW in the energy analysis and 13 % of the output, table 3.4. .

The exergy destruction in the furnace is about 46.5 MW and the exergetic efficiency, based on the fact that the metal is the only product, is about 30 %. If energy would be recovered by any means, e.g. electricity production, the exergetic efficiency would

Energy type	\dot{E}_{ph}	\dot{E}_0	$\dot{E}_0 + \dot{E}_0$	Part
Exergy in product	2.6 MW	29.5 MW	32.1 MW	62 %
Exergy in off-gas	16.9 MW	1.5 MW	18.4 MW	35.5 %
Cooling System	1 MW	0	1 MW	2 %
Directly from furnace	0.2 MW	0	0.2 MW	0.5 %

Table 3.6: Estimated exergy from furnace 3 in Elkem Iceland

increase. In figure 3.5 a Grassmann diagram is presented which shows the exergy streams graphically.

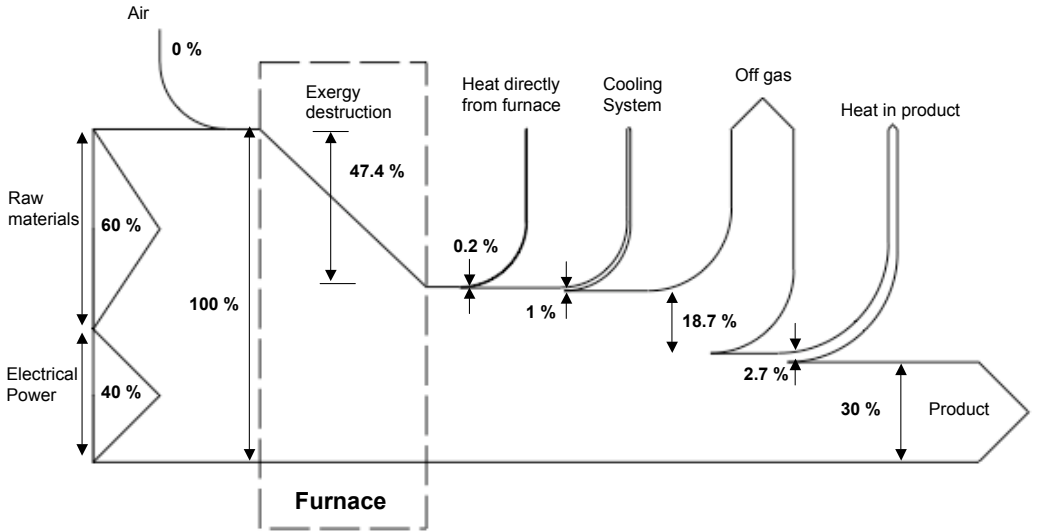


Figure 3.5: A Grassmann diagram of furnace 3 at Elkem Iceland Grundartangi based on the calculated results from the model. The ratio of the streams are based on the input.

If an energy recovery system were to be designed, considerations should be taken for a different kind of cooling system which would operate at higher temperature, in evaporative cooling or in a cooling system which allows for hotter water. With evaporator cooling though, more strain is put on the furnace equipment, as it is has to endure higher temperatures which will shorten the lifetime of the furnace [4].

4 Utilization

There are many options for utilizing the heat from the furnace at Elkem Iceland. In order to get an overview of the options available for heat recovery a functional analysis was performed and it is illustrated graphically in figure 4.1 [16].

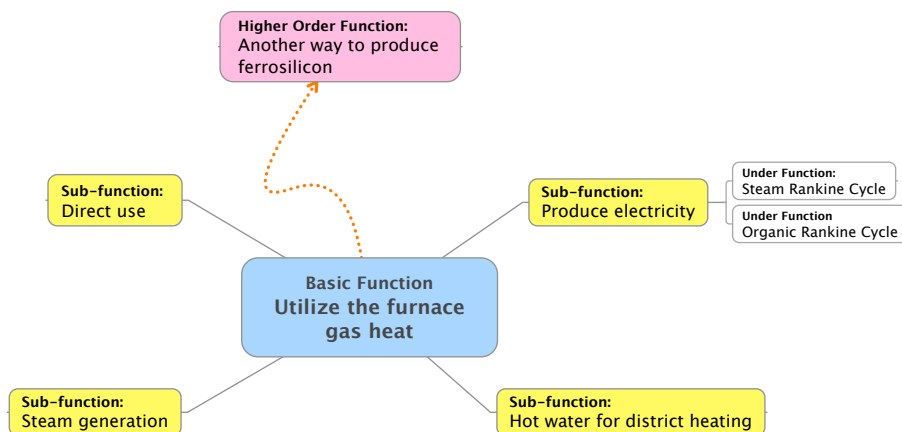


Figure 4.1: A functional analysis of the problem of heat recovery at Grundartangi

The main problem or the basic function is to utilize the heat from the process. A higher order function is defined as a solution that makes the basic function obsolete. In this case the higher order function is to use another way to produce ferrosilicon and make heat recovery unnecessary. The sub-functions are solutions to the basic function and they are: to produce steam, hot water for district heating, direct use and electricity production. The under functions for the electricity production are to use a typical steam Rankine cycle or an Organic Rankine Cycle. The main focus will

be on the sub-functions for electricity production.

One might think that one sub-function would be to utilize the heat to preheat the materials fed to the furnace, as is done in electric arc furnaces in steel industry. But that kind of heat recovery for FeSi furnace is not an feasible because a cold furnace top is preferable [37].

4.1 Electricity production

To convert heat to work we need to use a heat engine. Theoretically the furnace gas could be led through a Brayton-Cycle and it could be an alternative to the Rankine cycle as mentioned in [37]. This option is possible if the furnace gas where clean but it is not possible because the gas is very dirty and has condensing elements in it. The most practical way to convert this heat to work is to use a Rankine Cycle. Such a recovery system is shown in figure 4.2 in its simplest form. It starts with the heat recovery boiler which transfers heat from the waste heat stream to the Rankine cycle working fluid. The working fluid leaves the boiler as saturated or superheated vapor and is expanded in the turbine, where the enthalpy of the working fluid is dropped. Power is extracted and a generator produces electricity. The working fluid is then passed on to a condenser. The condenser condenses the working fluid to liquid and a feed pump raises the pressure and resupplies the boiler with fluid. The heat from the condenser is rejected to a cooling media which could be air or water. Grundartangi is placed by the sea and therefore it is ideal to utilize it as heat sink.

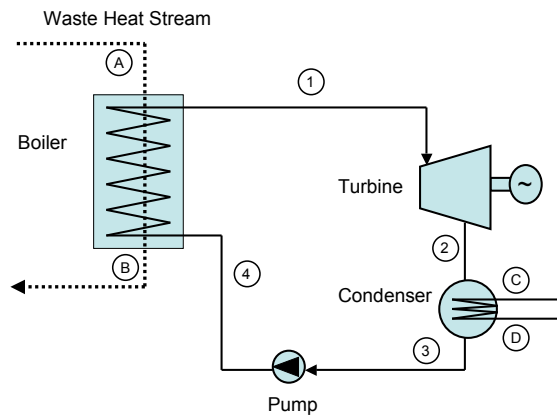


Figure 4.2: A schematic of a simple Rankine working cycle

4.1.1 Thermodynamics of Rankine cycle

Using the steam Rankine cycle is the common practice in ferrosilicon heat recovery [39]. The notation in the following equations are the same as in 4.2 where a schematic of a Rankine cycle is illustrated. The same thermodynamic equations are used for all working fluids, water or organic fluids and therefore only the thermodynamic relations for a simple Rankine cycle will be described. The only difference is the complexity of the whole system when these components are put together. The thermodynamic model is ideal and does not account for heat- or friction losses, although it accounts for entropy generation in the turbine and feed pump.

Boiler

In this thermodynamic model the boiler is assumed to be a counter flow heat exchanger. The energy balance of the boiler is:

$$(h_1 - h_4) \cdot \dot{m}_{wf} = (h_A - h_B) \cdot \dot{m}_{WHS} \quad (4.1)$$

where \dot{m}_{WHS} and \dot{m}_{wf} are the mass flow of the waste heat stream and the working fluid, h_A and h_4 are the enthalpy of the waste heat stream and working fluid entering the boiler and h_B and h_1 are the enthalpies of the waste heat stream and working fluid exiting. The temperature of the waste heat stream can never be lower than the temperature of the working fluid in any specific point in the boiler. This is called pinch and is usually defined as $\Delta T = 5^\circ \text{C}$. To estimate the heat exchanger size the heat exchanger can be cut into small elements and the following relation used:

$$dA = \frac{dq}{U \cdot \Delta T} \quad (4.2)$$

where dA is the heat transfer area, dq is the heat transferred, U is the heat-transfer coefficient and ΔT is the temperature difference.

Turbine

The working fluid generates work, \dot{W}_t , as it passes through the turbine. The work produced can be calculated by following equation:

$$\dot{W}_t = \dot{m}_{wf} \cdot (h_1 - h_2) \quad (4.3)$$

where h_1 is the enthalpy of working fluid entering the turbine and h_2 is the enthalpy of the fluid exiting.

An ideal turbine is described by an isentropic process but a real turbine has some increase in entropy and has an isentropic efficiency which is the ratio between actual work and isentropic work and is defined as following:

$$\eta_t = \frac{h_1 - h_{2a}}{h_1 - h_{2s}} \quad (4.4)$$

where h_{2a} is the actual enthalpy and h_{2s} is the isentropic enthalpy (if $s_1 = s_2$). The quality of the fluid is important if a wet liquid is used. For steam the quality cannot be lower than 85 % because the turbine cannot handle more moisture. The total electricity generated will then be

$$\dot{W}_e = \eta_g \cdot \dot{W}_t \quad (4.5)$$

where η_g is the generator efficiency typically 95% [5].

Condenser

The condenser is assumed to be a counter flow heat exchanger and the source for cooling fluid is the sea. The mean temperature of the sea near Hvalfjörður is 5 °C, mean temperature measurement in Hvalfjörður are not available. The energy balance of the condenser is:

$$(h_2 - h_3) \cdot \dot{m}_{wf} = (h_C - h_D) \cdot \dot{m}_{cf} \quad (4.6)$$

where \dot{m}_{cf} is the mass flow of the cooling fluid, h_C is the enthalpy of the cooling fluid entering the heat exchanger and h_D is the enthalpy of the cooling fluid exiting.

Feed Pump

The pump increases the pressure of the working fluid and is supplied by work. The work needed to increase the pressure of the fluid, \dot{W}_p , can be calculated by following equation:

$$\dot{W}_p = \dot{m}_{wf} \cdot (h_4 - h_3) \quad (4.7)$$

where h_3 is the enthalpy of the fluid entering the pump and h_4 is the enthalpy of the fluid exiting the pump. An ideal pump undergoes an isentropic process but an actual pump generates entropy. Isentropic efficiency for pump can be calculated with following equation:

$$\eta_p = \frac{h_{4s} - h_3}{h_{4a} - h_3} \quad (4.8)$$

where h_{4a} is the actual enthalpy and h_{4s} is the isentropic enthalpy. The feed pump efficiency is assumed to be $\eta_p = 50\%$ which is similar to what is found in geothermal power plants [28].

Efficiency

The thermal efficiency of a Rankine cycle is determined from:

$$\eta_{th} = \frac{\dot{W}_t}{\dot{Q}_{in}} \quad (4.9)$$

where \dot{Q}_{in} is the thermal energy into the system. This efficiency is based on the first-law of thermodynamics and makes no reference to the best possible performance and can be misleading. The second-law efficiency is more descriptive and is the ratio between the actual thermal efficiency and the maximum possible thermal efficiency, $\eta_{th,max}$, or carnot efficiency and can be expressed as:

$$\eta_{II} = \frac{\eta_{th}}{\eta_{th,max}} \quad (4.10)$$

This definition does not account for pressure. To account for pressure, the second law efficiency can be determined from exergy as:

$$\eta_{II} = \frac{\text{Exergy recovered}}{\text{Exergy supplied}} = 1 - \frac{\text{Exergy destroyed}}{\text{Exergy supplied}} \quad (4.11)$$

4.1.2 Modeling and optimization

The modeling software was developed using MATLAB [1] and the thermodynamic data originates from REFPROP [32]. The optimization software used is an evolutionary optimization algorithm developed by Thomas Philip Runarsson and Xin Yao [34]. The modeling does not account for heat- and friction losses in pipes and equipment.

4.1.3 Steam Rankine working cycle

A steam Rankine cycle design for heat recovery at Grunadartangi is shown in figure 4.3. The only difference from the simple Rankine cycle presented in figure 4.2 is the use of heat from the Cooling System (CS) to heat up the working fluid before the boiler. The mass and energy balance for this extra component is similar as in the condenser and boiler:

$$(h_5 - h_4) \cdot \dot{m}_{wf} = (h_G - h_H) \cdot \dot{m}_{cs} \quad (4.12)$$

where the \dot{m}_{cs} is the mass flow used in the heat recovery and h_G and h_H the enthalpy of the streams of the CS going in and out of the heat exchanger. From the measurements in appendix A it was found that the mass flow of the CS was $\dot{m}_{CS} = 420$ kg/s and the temperature drop in the heat exchanger was from about $T_G = 50^\circ\text{C}$ to about $T_H = 40^\circ\text{C}$. This restriction is applied in the designed steam Rankine cycle. It is obvious that this energy is of low quality and not all will be used by the Rankine cycle and most of it has to be rejected. The CS could be redesign to produce superheated steam as is done in Thamshavn [39] which would call for a redesign and expensive reconstruction of the furnace smoke head.

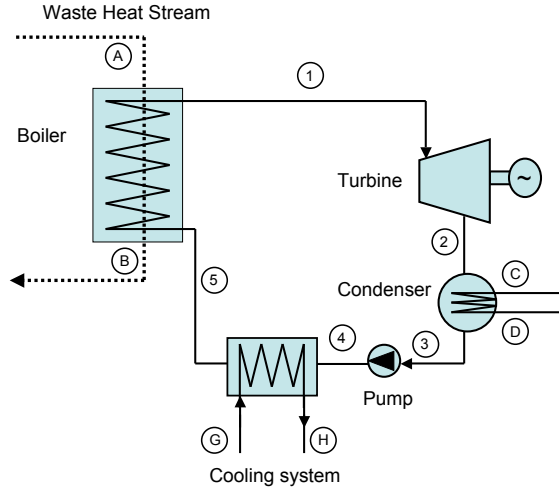


Figure 4.3: A schematic of system setup for steam Rankine working cycle for heat recovery at Grundartangi

4.1.3.1 Optimization and constraints

No heat- or friction losses are accounted for, efficiency of turbine is assumed to be $\eta_t = 85\%$ and efficiency of pump $\eta_p = 50\%$. The objective of the optimization is to maximize the power output from the power plant by varying the temperature and pressure of the steam exiting the boiler. The fitness function and the constraints of the optimization parameters are:

$$f(t_1, p_1) = \dot{W}_t - \dot{W}_p \quad (4.13)$$

$$200 \leq t_1 \leq 445 \text{ [}^\circ\text{C]} \quad (4.14)$$

$$1000 \leq p_1 \leq 5000 \text{ [kPa]} \quad (4.15)$$

where t_1 and p_1 is the temperature and pressure exiting the boiler. Other constraints are:

- Steam quality can not be lower than 85 %
- Pinch in all heat exchangers can not be less than $\Delta = 5^\circ\text{C}$
- Furnace gas is fixed at 450°C down to 220°C

- Condenser pressure is fixed at 5 kPa and is restricted by the turbine size

4.1.3.2 Results for steam Rankine cycle

The optimization was done for both the special steam Rankine cycle in figure 4.3 and the simple steam Rankine cycle in figure 4.2 for comparison. The resulting states in the cycles are presented in table 4.2 and a comparison of key parameters of the cycles in table 4.1. The TS diagram for the special steam Rankine is in figure 4.4 and the temperature profile of the heat exchanges in the for the same cycle are shown in figure 4.5.

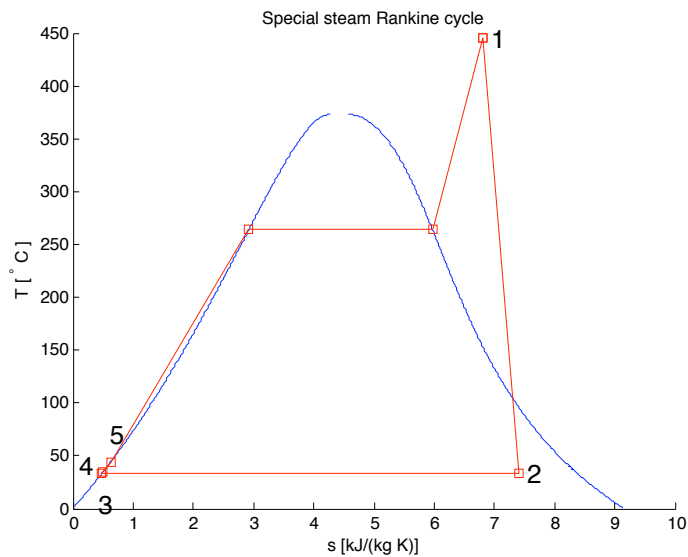


Figure 4.4: A TS diagram of the optimum state for the special Steam Rankine cycle. The point for states 3 and 4 are nearly concentric.

	f [MW]	η_{th} [%]	η_{II} [%]	\dot{m}_{wf} [kg/s]	\dot{m}_{cf} [kg/s]	\dot{m}_{CS} [kg/s]	\dot{Q}_{CON} [MW]	\dot{Q}_{CS} [MW]
Simple Rankine	7.92	32.9	60.4	7.57	171.4	—	16	—
Rankine with CS	7.96	32.8	58.7	7.69	174	7.89	16.3	0.33

Table 4.1: The key parameter of the optimum solution for the working cycles

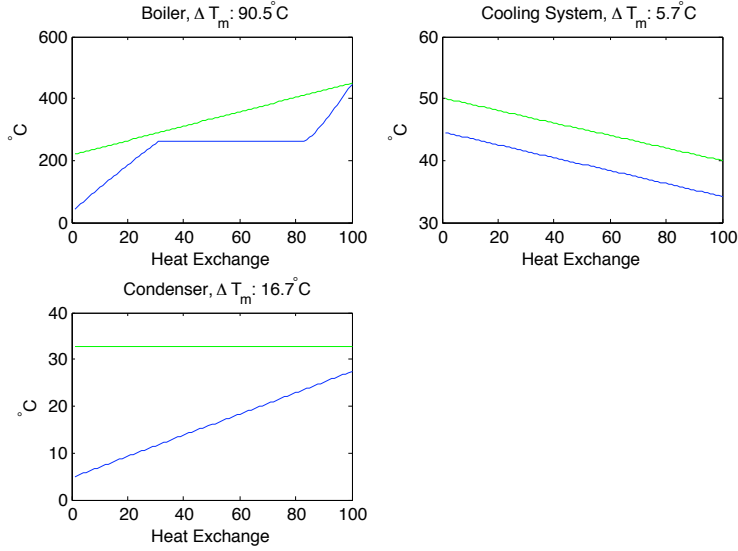


Figure 4.5: The temperature profiles of the Boiler, Cooling System and Condenser for the special steam Rankine cycle

Point	1		2		3		4		5	
	T	P	T	P	T	P	T	P	T	P
Simple Rankine	445	5000	32.9	5	32.9	5	34.2	5000	—	—
Rankine with CS	445	5000	32.9	5	32.9	5	34.2	5000	44.5	5000

Table 4.2: The state of the working fluid in the optimum configuration T is in $^\circ\text{C}$ and P is in kPa

The maximum net power output for simple Rankine cycle and the special Rankine cycle are 7.92 MW and 7.96 MW respectively. The benefit of using the CS for preheating are negligible and difference in net power production is less than 1 %. The energy used from the Cooling System is only 0.33 MW of the total 13 MW that are available. Therefore most of the energy in the CS has to be thrown away and the contribution to electricity production is small. The use of the CS also results in a drop both in the thermal efficiency and the second law efficiency. The main reason for this behavior is that the temperature of the heat supplied by the CS is low, but it is nevertheless heat and comes as an input into equation 4.9 and 4.11. Higher efficiency is related to the higher temperatures of the heat source. If the CS would be redesigned and higher temperatures available the effect on the working cycle would

be good because then it would serve better as a preheater before the boiler.

4.1.4 Organic Rankine Cycle

The setup of an Organic Rankine Cycle is a little bit more complicated than the steam Rankine design shown in figure 4.3, but the thermodynamic relations are the same. Because of the saturation vapor curve of the organic fluid there is no need to set the constraint about the quality of the vapor exiting the turbine as with steam as working fluid. The vapor always leaves the turbine in superheated state. Three cases of an Organic Rankine Cycle are designed for heat recovery at Grundartangi. Case one is illustrated in figure 4.6 and does not utilize the heat from the Cooling System, but has a recuperator.

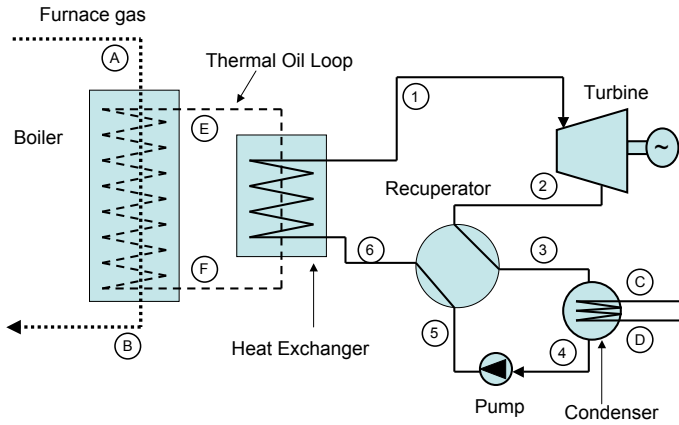


Figure 4.6: A schematic of an Organic Rankine cycle for heat recovery at Grundartangi, design case one

Because the organic fluid is flammable the need for thermal oil loop rises which isolates the working fluid from the furnace gas. This loop has thermal oil which flows through the furnace gas heat exchanger and then boils the organic fluid in another heat exchanger. The thermodynamic relations for this extra loop are:

$$(h_A - h_B) \cdot \dot{m}_{OG} = \dot{m}_{oil} \cdot c_p \cdot (T_E - T_F) \quad (4.16)$$

where \dot{m}_{oil} is the mass flow of the thermal oil, c_p is specific heat of the thermal oil and the T_E and T_F are the temperature at the exit and inlet of the heat exchanger.

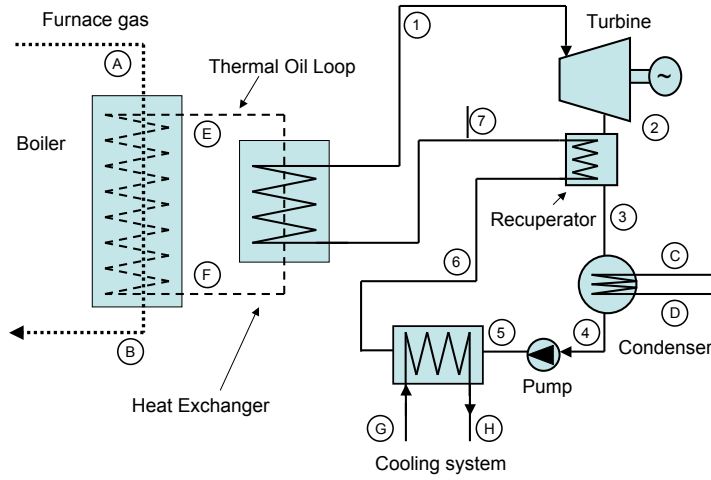


Figure 4.7: A schematic of an Organic Rankine cycle for heat recovery at Grundartangi, design case two

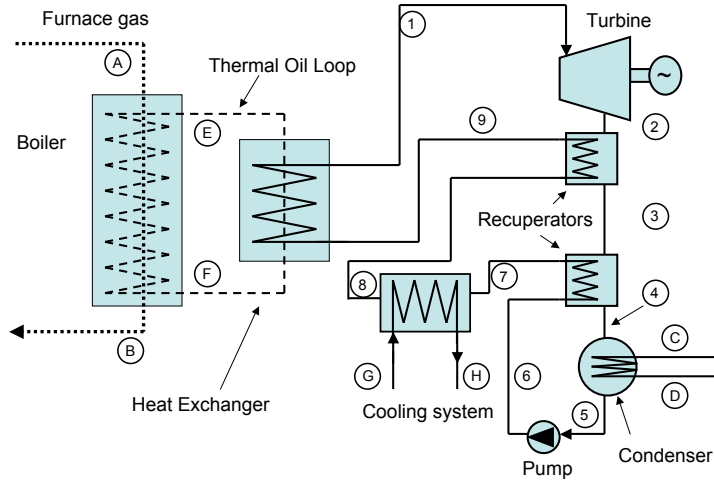


Figure 4.8: A schematic of an Organic Rankine cycle for heat recovery at Grundartangi, design case three

The specific heat is chosen as $c_p = 2.0 \text{ kJ/kg}^\circ\text{C}$ [14]. The temperature of the thermal loop are set as close to the furnace gas temperature as the pinch allows, because of the risk of condensation of sulphuric acid. The recuperator utilizes the vapor that exits

the turbine to heat up the working fluid going to the boiler. The thermodynamic relation for the recuperator are:

$$(h_2 - h_3) \cdot \dot{m}_{wf} = (h_6 - h_5) \cdot \dot{m}_{wf} \quad (4.17)$$

where h_2 and h_5 are the enthalpies of the streams entering the recuperator and h_3 and h_6 are the enthalpies of the streams exiting. The equation can be simplified as the mass flow of the working fluid cancels out. The pinch in a recuperator with organic fluid is assumed $\Delta T = 8^\circ\text{C}$.

Case two is shown in figure 4.7 and has the CS included as a preheater after the condenser and before the second preheating. As in the steam Rankine cycle, the CS has its restrictions and has the same thermodynamic relations as in equation 4.17 but different subscripts as illustrated in figure 4.7.

Case three is shown in figure 4.8 and has two recuperators between the CS and has similar thermodynamic relations as the other two cases but different subscripts which are illustrated in figure 4.8.

4.1.4.1 Fluid selection

The fluids selection is restricted to the fluids that are available in REFPROP. The most feasible ones for these temperatures are Toluene and Benzene. They are also proven as working fluids in ORC applications [8]. Their properties are listed in table 4.3. Toluene is chosen as working fluid as it shows higher critical temperature than Benzene and it can sustain higher temperatures and pressure. Water is included in the table for comparison.

	Toluene	Benzene	Water
Chemical Formula	C_7H_8	C_6H_6	H_2O
Molecular weight [kg/kmole]	92.1	78.1	18
T_{crit} [$^\circ\text{C}$]	318.6	288.9	374
P_{crit} [MPa]	4.1	4.9	22.06
T_{max} [$^\circ\text{C}$]	426.85	361.85	–
P_{max} [MPa]	500	78	–
Normal Boiling point [$^\circ\text{C}$]	110.6	80.08	100

Table 4.3: Thermodynamic properties of working fluids [32]

4.1.4.2 Optimization and constraints

For all the cases no heat- or friction losses are accounted for, efficiency of turbine is assumed $\eta_t = 85\%$ and efficiency of pump $\eta_p = 50\%$. The objective of the optimization is to maximize the power output from the power plant by varying the optimization parameters. Other constraints are the same in all cases and are:

- Pinch in heat exchangers can not be less than $\Delta = 5^\circ\text{C}$ but pinch in the recuperators is not less than $\Delta = 8^\circ\text{C}$
- Furnace gas temperature is fixed at 450°C down to 220°C
- The temperature of the water exiting the condenser is $T_D = 20^\circ\text{C}$

Case One

The fitness function for case one is:

$$f(t_1, p_1, p_2) = \dot{W}_t - \dot{W}_p \quad (4.18)$$

$$200 \leq t_1 \leq 425 [^\circ\text{C}] \quad (4.19)$$

$$1000 \leq p_1 \leq 5000 [\text{kPa}] \quad (4.20)$$

$$0 \leq p_2 \leq 30 [\text{kPa}] \quad (4.21)$$

where t_1 and p_1 are the temperature and pressure exiting the boiler and p_2 is the pressure of the condenser.

Case Two

The fitness function for case two is:

$$f(t_1, p_1, p_2, t_3) = \dot{W}_t - \dot{W}_p \quad (4.22)$$

$$200 \leq t_1 \leq 425 [^\circ\text{C}] \quad (4.23)$$

$$1000 \leq p_1 \leq 5000 [\text{kPa}] \quad (4.24)$$

$$0 \leq p_2 \leq 30 [\text{kPa}] \quad (4.25)$$

$$25 \leq t_3 \leq 200 [^\circ\text{C}] \quad (4.26)$$

where t_3 is the temperature in point three in figure 4.7, that is the temperature of the working fluid after the turbine.

Case Three

The fitness function for case three is:

$$f(t_1, p_1, p_2, t_4, tt) = \dot{W}_t - \dot{W}_p \quad (4.27)$$

$$200 \leq t_1 \leq 425 \text{ [}^\circ\text{C]} \quad (4.28)$$

$$1000 \leq p_1 \leq 5000 \text{ [kPa]} \quad (4.29)$$

$$0 \leq p_2 \leq 30 \text{ [kPa]} \quad (4.30)$$

$$25 \leq t_4 \leq 200 \text{ [}^\circ\text{C]} \quad (4.31)$$

$$25 \leq tt \leq 200 \text{ [}^\circ\text{C]} \quad (4.32)$$

where t_4 is the temperature in point 4 in figure 4.8, that is the temperature of the working fluid before the condenser. The variable tt defines the temperature in point 3 by $t_3 = t_4 + tt$ and automatically sets one extra constraint, that is $t_3 > t_4$.

4.1.4.3 Results for ORC

The optimization was done for each case and the results are listed in table 4.4 and the states of the optimal solutions shown in table 4.5. Case Two has the highest net power output of 9.82 MW, second Case One with 9.74 MW and last Case Three with 6.88 MW. In figure 4.9 a T-S diagram of Case Two ORC is shown and in figure 4.10 the temperature profiles of the heat exchangers in the same system are shown. The optimum solution of all the cases resulted in supercritical working cycle as seen in figure 4.9. The benefit of using the CS to preheat the working fluid is about 100 kW, that is the difference between Case One and Two. Case Three is over designed and the pinch restrictions in the second recuperator are the reason this configuration is much worse than the other. Because of the pinch the system has to perform heat exchange in the second recuperator which leads to less performance. The CS is better utilized by the ORC cycle than the steam Rankine because the temperature limit fits better into the system before the recuperator.

One interesting result from the optimization is that the pinch in the boiler for the ORC configurations finds its optimum in the middle, as seen in figure 4.10. Usually the pinch restriction will be at the exit of the working fluid so the temperature is at

maximum as seen in the optimization of the Rankine cycles. This is clearly illustrated in figure 4.5 were the temperature profile of the heat exchangers of the special Rankine system are shown and the pinch is at the exit of the boiler.

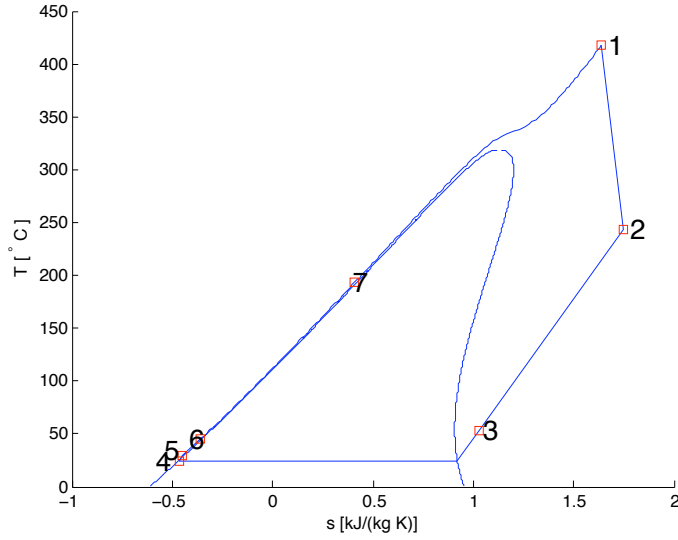


Figure 4.9: The TS diagram for configuration in Case Two

	f [MW]	η_{th} [%]	η_{II} [%]	\dot{m}_{wf} [kg/s]	\dot{m}_{cf} [kg/s]	\dot{m}_{CS} [kg/s]	\dot{Q}_{CON} [MW]	\dot{Q}_{CS} [MW]
ORC Case One	9.74	40.7	74.71	33.2	225.8	—	14.2	—
ORC Case Two	9.82	39.5	72.4	33.6	239.4	22.4	15.1	0.94
ORC Case Three	6.88	28.1	50	26.9	214	12.9	13.5	0.54

Table 4.4: The key parameters of the optimum solution for the working cycles

4.1.5 Steam Rankine vs. Organic Rankine

The optimal solution for the ORC produces about nearly 2 MW more net power than the steam Rankine cycle and the second law efficiency is about 13 % higher. The fact that the organic vapor leaving the turbine is superheated and that it can be used in a recuperator to heat up the fluid entering the boiler, gives the ORC a big advantage. The lower temperature of the furnace gas is restricted to 220 °C and therefore the

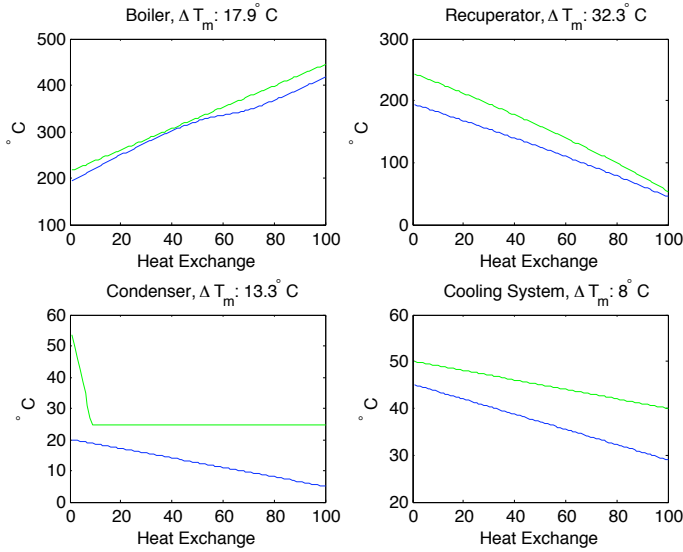


Figure 4.10: The temperature profiles of the Boiler, Cooling System and Condenser for the special steam Rankine cycle

	ORC Case One ([°C],[kPa])	ORC Case Two ([°C],[kPa])	ORC Case Three ([°C],[kPa])
Point 1 (T,P)	(420, 5000)	(417.6, 5000)	(364, 5000)
Point 2 (T,P)	(245.5, 3.7)	(243, 3.7)	(177, 3.3)
Point 3 (T,P)	(37.5, 3.7)	(53.5, 3.7)	(98.4, 3.3)
Point 4 (T,P)	(24.5, 3.7)	(29, 3.7)	(90, 3.3)
Point 5 (T,P)	(29, 5000)	(24.5, 3.7)	(21.7, 3.3)
Point 6 (T,P)	(191, 5000)	(45, 5000)	(26.2, 5000)
Point 7 (T,P)	(-, -)	(193.4, 5000)	(33, 5000)
Point 8 (T,P)	(-, -)	(-, -)	(44.5, 5000)
Point 9 (T,P)	(-, -)	(-, -)	(109, 5000)

Table 4.5: The state of the working fluid in the optimum configuration

steam Rankine Cycle has to use this high temperature, and high quality energy, to heat the water in the working cycle from 45 °C to the optimum point. The ORC on the other hand has its working fluid preheated with the recuperator and therefore the temperature of the fluid entering the boiler is much higher or about 193 °C and less of the quality of energy is lost. Another factor is that the ORC working fluid

has lower critical pressure and temperature than the water and can therefore get supercritical cycle within the pressure limits set in the optimization. In figure 4.11 the temperature profile is shown for the boiler in the steam Rankine Cycle and the ORC Case Two.

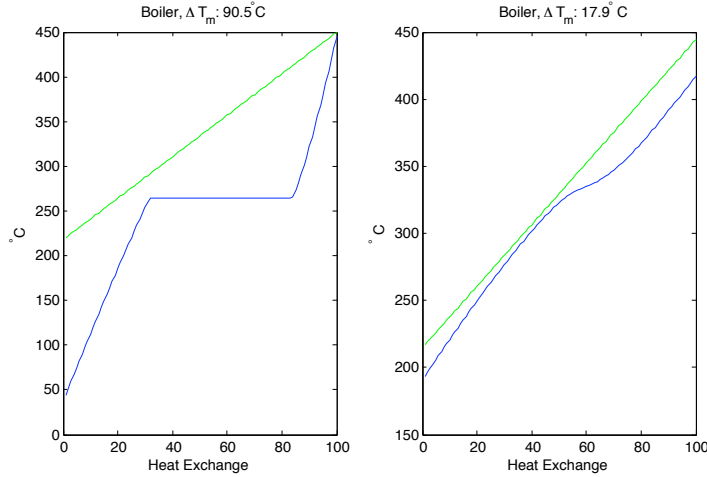


Figure 4.11: The temperature profile in special steam Rankine cycle (left) and ORC Case Two(right).

It can be seen that the temperature of the ORC working fluid "follows" the furnace gas better than the steam. The mean temperature difference of the boiler in the steam Rankine is $\Delta T_m = 90.5^\circ\text{C}$ while in the ORC boiler it is $\Delta T_m = 17.9^\circ\text{C}$. This leads to less entropy generation which is determined by the temperature difference of the two streams.

To get better utilization of the energy, it should be considered to change the Cooling System because it has the potential to deliver higher quality energy. The temperatures in the CS are even not high enough to use in district heating. That will be shown by the fact that all the configurations of working cycles use less than 1 MW of the 13 MW available in the cooling system.

4.2 Other utilizations

From a thermodynamic point of view the best way to recover heat is to utilize it for heating purposes. This could be e.g. agriculture, fish farming, heat for greenhouses,

steam generation for industry and hot water generation for district heating. Here the steam generation and hot water production will be looked at closer.

To utilize the heat from the furnace we use the heat from the Cooling System (CS) to preheat the water and then a heat exchanger with the furnace gas (OG) to heat the water up to the temperature needed. A schematic of this setup is illustrated in figure 4.12 and is this similar for both cases, just with different temperatures and pressures.

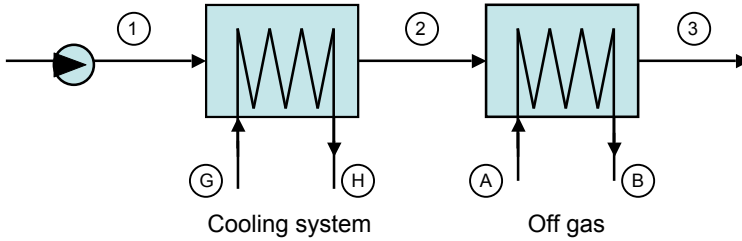


Figure 4.12: A schematic of hot water and steam production.

4.2.1 District heating

There are two heat sources available, one in the cooling system (CS) and one in the furnace gas (OG). The CS is used to preheat the water and the OG then heats it up to the temperature of the district heating which is $80\text{ }^{\circ}\text{C}$. The same thermodynamic relations are valid as for the CS and OG in the Rankine cycle. The mass flow of water was maximized using iteration. The assumptions are following:

- The temperature of the water available is $T_1 = 5\text{ }^{\circ}\text{C}$
- The district heating system is designed as $80/40/-10$ ¹
- The output temperature is $T_3 = 80\text{ }^{\circ}\text{C}$

¹80/40/-10 is abbreviation. Feedwater is $80\text{ }^{\circ}\text{C}$, backwater is $40\text{ }^{\circ}\text{C}$ and the DH system is designed for maximum load at $-10\text{ }^{\circ}\text{C}$ air temperature.

The maximum mass flow obtained when the temperature between the heat exchangers was $T_2 = 36^\circ\text{C}$ and is therefore :

$$\dot{m}_{DH} = 134.5 \text{ kg/s} \approx 11800 \text{ m}^3/\text{day} \quad (4.33)$$

This is 80°C hot water which can supply a district heating system with the heat load of $\dot{Q}_{DH} = 22.5 \text{ MW}$. The temperature profiles in the heat exchangers are illustrated in figure 4.13 and from the mean temperature in the heat exchanged with the furnace gas, $\Delta T = 277.9^\circ\text{C}$, it is obvious that a high entropy generation is taking place and therefore exergy destruction will occur by producing hot water from high temperature furnace gas.

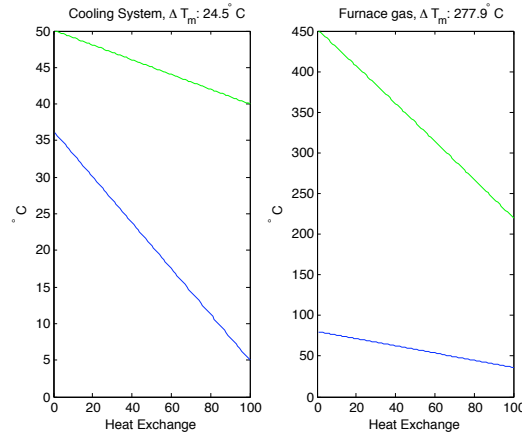


Figure 4.13: The temperature profile in the heat exchangers to produce hot water

To put this figures in perspective a closer look at Akranes, which is a town about 15 km from Grundartangi is performed. Akranes gets its hot water for district heating from Deildartunguhver, which is located about 75 km from Akranes. The supply pipe is therefore probably the longest supply pipe of hot district heating water in world [33]. The daily mean hot water usage in Akranes for the year 2007 is illustrated in figure 4.14 [36]. As seen there the maximum load during the winter months does not exceed $9000 \text{ m}^3/\text{day}$ and therefore could the hot water production from Grundartangi could supply all the hot water demand of Akranes today and also in the near future.

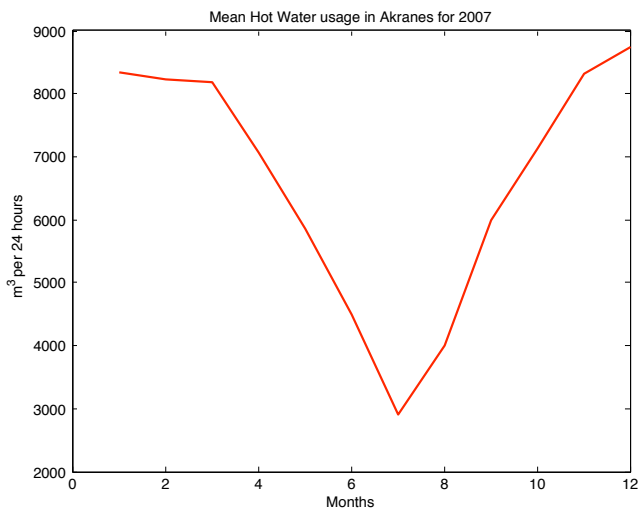


Figure 4.14: The mean hot water usage in Akranes for each month in the year 2007 [36]

4.2.2 Steam generation

Steam is used in large quantities in industries and one possibility of utilizing the heat from the furnace is to generate steam. The system configuration in figure 4.12 is used when steam is generated as with the district heating. The water is preheated in the CS and then superheated in heat exchanger with the furnace gas. When producing steam, only part of the CS is utilized because the limiting factor is the heat exchange with the furnace gas. In figure 4.15 the amount of steam at various pressure is shown and has a capacity in the range of 8 to 9 kg/s depending on the temperature and pressure needed.

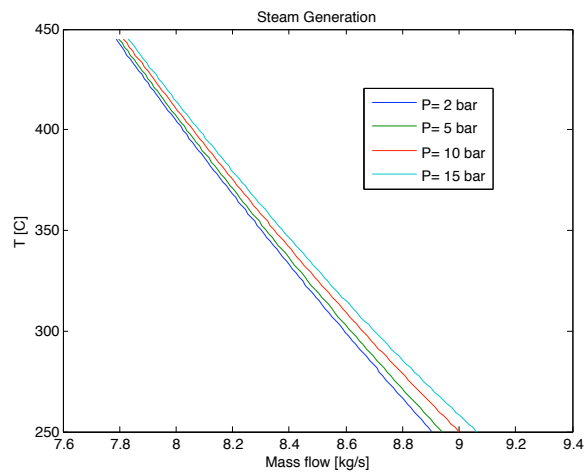


Figure 4.15: Mass flow of steam vs. temperature of selected pressures for steam generation

5 Economic analysis

There are several ways of conducting a cost estimate and they depend on the level of detail and effort. One method is to start from the bottom and design each component and estimate its size. Then get vendors quotation for the price of the component based on the size estimated and find the total purchase equipment cost. From the total purchased equipment cost, the total capital investment and operational and maintenance cost can be estimated.

Another way is to conduct an economic analysis is the top down approach. The top down approach uses existing plant of similar kind to estimate the capital cost of the proposed plant. This method is described in the following chapters.

The capital cost and levelized cost of electrical energy for the special steam Rankine cycle and the ORC configuration in case two is estimated and will be referenced to as just steam Rankine and ORC in the following text. As this is just a preliminary economic estimate, the power cycles will be evaluated only on the net power base. Although the ORC will be evaluated with bottom up method and quotations from an expend in the field of geothermal energy utilization to increase accuracy.

5.1 Capital Cost of Power Plants in Iceland

To estimate the average total capital cost by the top down approach it is essential to know the cost of similar projects [2] and it is preferable to use figures that are not too old. The installed electric power production capacity in Iceland is mostly hydropower (74.4 %) and secondly geothermal (20.5 %) and a small fraction of the

installed capacity comes from oil (5.2 %) utilized in remote areas [27]¹. In Iceland the trend for electricity production has been moving from hydropower to geothermal and there are several geothermal power plants on the drawing board. The most recent hydropower plant in Iceland is Kárahnjúkavirkjun, placed in the east of Iceland, which is owned and operated by Landsvirkjun. It was constructed in the years from 2003 to 2007 and has an installed capacity of 690 MWe and produces about 4660 GWh per year. The estimated total cost of this project, according to Landsvirkjun in september 2007 [22], was 133 307 million ISK which is roughly 193.2 million ISK per MW. The electricity from Kárahnjúkavirkjun is all sold to Alcoa Fjarðarál which produces aluminum.

Another power plant project under construction is Hellisheiðarvirkjun, which is a geothermal power plant in the south-west of Iceland on an active volcanic ridge. It is owned by Orkuveita Reykjavíkur (OR) and its current capacity is 213 MWe. Estimated final production capacity will be 300 MWe and 400 MWth. According to OR [13] the average price for CHP is 150 million ISK per MWe [13]. This figure includes boreholes and investment cost and the cost per MWe is so low because the plant combines electricity production and district heating. OR has two other geothermal power plants planned in the same region as Heilisqueiðarvirkjun. One of these two is Bitruvirkjun which will only produce electricity. The average price for geothermal electricity production is 180 millions per MWe [13]. Only about one year ago this price estimate was in 200 millions per MWe but has gone down because of lower material prices. A summary of this is in table 5.1 .

Power Plant	Type	Electricity	Thermal	Cost per MWe
–	–	MWe	MWth	10 ⁶ ISK/MWe
Hellisheiðarvirkjun	CHP	300	400	150
Bitruvirkjun	Electricity	135	0	180

Table 5.1: Estimated capital cost of geothermal power plant projects in Iceland[13, 33]

For comparison with the figures in table 5.1, the company Kaldara Green Energy is selling their single flash geothermal power plants units without drilling costs on \$ 1 350 000 per MWe [18] or about 162 millions ISK per MWe². Their system could be used at Grundartangi but it does not include a boiler or a condenser using sea water and they haven't sold any units yet.

¹In the year 2007

²Exchanges rates 3. March 2009, 120 ISK/\$

5.2 Estimation of Capital Cost for Waste Heat Recovery

A geothermal power plant is similar to a waste heat recovery plant. They both use Rankine cycle and from thermodynamic point of view the only difference is that in the geothermal one the heat is supplied from boreholes in an open system but in the waste heat recovery it is a closed system and the heat is supplied from a furnace.

To estimate the capital cost of a waste heat recovery plant, scaling is used and the cost data from chapter 5.1. This method is based on the fact that when available average cost data of complete plants is plotted against their size on log-log plot, the data correlation results in a straight line, in a given capacity range. The slope of this line, α , is called scaling exponent and is given by the relation:

$$C_Y = C_W \cdot \left(\frac{X_Y}{X_W} \right)^\alpha \quad (5.1)$$

where C_Y is estimated average price of a proposed plant and X_Y its capacity, C_W is cost of a complete plant of same kind and X_W its capacity. The scaling exponent, α , for an electricity power plant is given in table 5.2 and also the α for cogeneration plant for comparison.

Plant	Capacity variable	Capacity range	α
Electricity power plant	Net power	1 - 1000 MW	0.80
Cogeneration plant	Net power	5 - 150 MW	0.75

Table 5.2: Typical values for scaling exponent, α [2]

From the quotation from OR, it is possible to estimate the capital cost of a waste heat recovery plant from the net power using equation 5.1. The estimated capital cost is presented in table 5.3 and this kind of estimate has the accuracy of about 50 % [12].

Cycle	Net power	Estimated Capital Investment
Steam Rankine	8 MWe	$2500 \pm 1250 \cdot 10^6$ ISK
ORC	10 MWe	$3000 \pm 1500 \cdot 10^6$ ISK

Table 5.3: Estimated Capital Investment for waste heat recovery

To get higher accuracy more effort has to be put in the accurate design of individual components and related costs as mentioned in the beginning. This estimate is though most probably an overestimate because of several factor that are different in a geothermal power plant. At the waste heat recovery the pressures are much higher and therefore smaller pipe diameters are required. Also, this is a closed system and the working fluid is clean, but in the geothermal plant the working fluid has impurities that cause scaling and corrosion problems. This fact allows for cheaper materials for pipings, etc. And at last, the waste heat recovery plant is built in a brownfield, that is new unit at existing site, while the geothermal power plants are built at a greenfield or new site with no service facilities such as roads and power lines.

5.3 Levelized cost of electrical energy

According to [29] levelized cost of the electricity produced in a waste heat recovery plant can be calculated by taking into account capital related costs, C_{CR} , and operating and maintenance cost (O&M), C_{OM} . The following relation can be used to calculate the levelized cost of electrical energy, first defining the C_{CR} as:

$$C_{CR} = \frac{\varphi}{8766 \cdot L} \cdot \left(\frac{I}{K} \right)_{-c} \cdot \left(1 + \frac{x+y}{2} \right)^c \quad (5.2)$$

where L is the plant capacity factor, φ is annual fixed charge rate, x is the discount rate, y is the annual rate of monetary inflation, c is the time to construct plant and the term $\left(\frac{I}{K} \right)_{-c}$ is overnight specific capital cost, that is the cost if the plant could be constructed overnight, and it is in ISK per kWe. For the O&M costs, C_{OM} , the relations are following:

$$C_{OM} = \frac{1}{8766 \cdot L} \cdot \left(\frac{O}{K} \right)_O \cdot \left(1 + \frac{y \cdot T}{2} \right)^c \quad (5.3)$$

where T is useful life of a plant in years and the term $\left(\frac{O}{K} \right)_O$ is the specific O&M cost as of start of operation in ISK per kWe. By summing the capital related costs and the O&M cost the total lifetime-levelized cost of electrical energy is estimated:

$$C_{tot} = C_{CR} + C_{OM} \quad (5.4)$$

5.3.1 Assumptions

The plant capacity factor, L , is the actual energy output of a power plant compared to the energy output if the plant always was at 100 % rated power. To give a little bit more realistic estimate 0.5 MW is subtracted from the net power calculated for service facilities, lighting, etc. as according to [12]. The assumption here is that the plant will be operated about 8500 hours per year which gives $L = 0.95$.

The discount rate is based on how capital is raised for financing the plant. It was assumed that 70 % of the capital would be raised by selling bonds, $b = 0.70$, and the rest would be covered by stock. The annual rate of return on the bonds is assumed to be 6 %, $r_b = 0.06$, and the return on stock to be 15 %, $r_s = 0.15$. The discount rate is therefore:

$$x = (1 - \tau) \cdot b \cdot r_b + (1 - b) \cdot r_s = 0.0807 \quad (5.5)$$

where τ is the tax fraction and in Iceland it is 15 %. From the discount rate the annual fixed charge rate can be calculated by following:

$$\varphi = x / (1 - \tau) = 0.095 \quad (5.6)$$

At the time of writing this the 12 month annual rate of monetary inflation in Iceland is about 18 %. To calculate with this temporary inflation is ridiculous and therefore the mean inflation for the past 6 years is used, which is 6 %. The time to construct a small scale plant as this is assumed to be 2 years and the lifetime of the plant can be assumed to be 30 years [12].

For the specific O&M cost a rule of thumb from the geothermal power plants was adapted. The rule of thumbs states that the cost related to O&M expenses are roughly 2 % of the total purchased equipment costs [10]. Another rule of thumb is used to estimate the purchased equipment cost which states that it is roughly 1/3 of the total capital cost. For the waste heat recovery the O&M cost might be smaller because of the difference in working fluids as mentioned earlier. The fluid in the geothermal plant is contaminated with minerals and in the heat recovery system the working fluid is clean. On the other hand the small size of the heat recovery capacity could counterbalance this fact and therefore the same rule of thumb used.

Based on these assumptions the lifetime levelized cost of electrical energy production can be calculated for the steam Rankine cycle and the ORC with equation 5.2 and 5.3 and the result is:

- Steam Rankine: $C_{tot} = 4.9 \pm 2.5$ ISK/kWh
- ORC: $C_{tot} = 4.6 \pm 2.3$ ISK/kWh

The reason the ORC has lower energy price per kWh is that in this estimate the cost of equipment is not accounted for and the ORC produces more kWh per year of the lifetime of the plant.

5.3.2 Sensitivity analysis

The sensitivity analysis determines the effect of changing individual input variable in the levelized cost estimate. The variable under consideration is changed by a percentage while other variables are kept constant. The variables chosen for the sensitivity analysis were: specific capital cost, $(\frac{I}{K})_{-c}$, specific O&M cost, $(\frac{O}{K})_O$, discount rate, x , and inflation, y . The result of the sensitivity analysis for steam Rankine cycle is presented in sensitivity graph in figure 5.1.

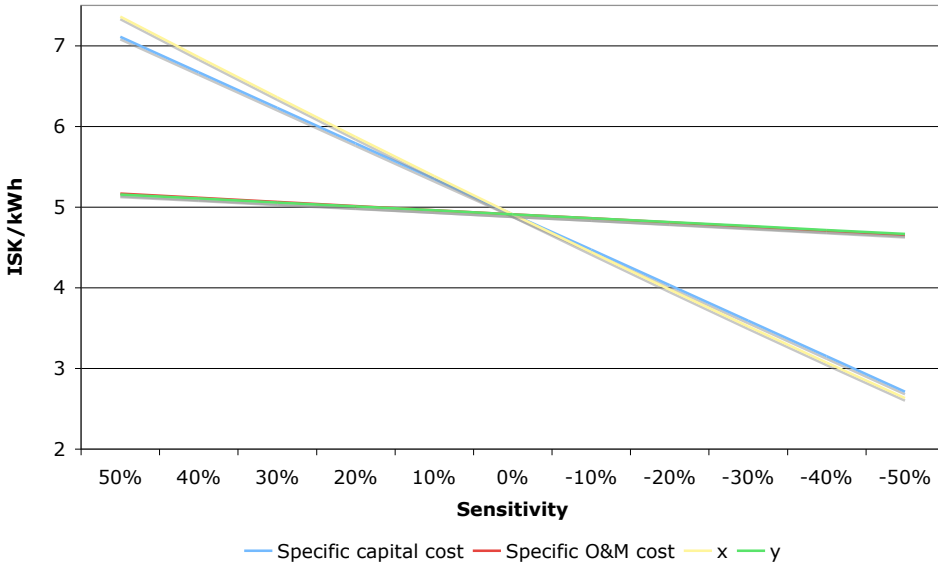


Figure 5.1: A sensitivity analysis for the levelized cost of electrical energy for steam Rankine cycle. Variables are: specific capital cost, $(\frac{I}{K})_{-c}$, specific O&M cost, $(\frac{O}{K})_O$, discount rate, x , and inflation, y .

There it can be seen that the specific O&M cost and the inflation have similar impact on the levelized cost. The specific capital cost and the discount rate also have similar

impact on the levelized cost but are obviously of greater importance than the other two as illustrated in figure 5.1. Therefore if a more accurate estimate of levelized cost of electrical energy is wanted, more attention should be paid to the specific capital cost and the discount rate. The sensitivity analysis for the ORC gave very similar results and the same variable are of importance as in the sensitivity analysis of the steam Rankine cycle.

5.4 More detailed analysis of the ORC

Because that the ORC cycle is different from the geothermal power plant a more detailed estimate will be performed for the ORC setup. For a more realistic estimate of the cost of the ORC power plant the pressure in the cycle is reduced below supercritical to subcritical which results in net power of 9.2 MW.

5.4.1 Heat exchangers

To estimate the size of the heat exchangers the overall heat-transfer coefficient has to be estimated. The overall heat-transfer coefficient is based on the convection of both size of the heat exchanger and the conduction through the material which separates the fluids. In many practical problems the conduction resistance is small compared with the convection resistance and therefore the convection on either side will dominate the heat-transfer. E.g. in the heat exchange between the furnace gas and water or oil the heat transfer at the gas side is dominating and therefore the overall heat-transfer coefficient is based on that restriction. The estimated overall heat-transfer coefficients are listed in table 5.4.

Component	Fluids	U	ΔT_m	\dot{Q}	A
-	-	[W/m ² K]	°C	MW	m ²
Thermal oil loop	Gas - Oil	100	30	23.9	7967
Boiler	Toluene - oil	1200	29	23.9	687
Condenser	Toluene - water	1200	13.3	15.8	990
Cooling system	Toluene - water	1200	8.9	1.1	103
Recuperator	Toluene - Toluene	1200	29.3	8.8	250

Table 5.4: Rough estimation of the overall heat-transfer coefficient [5, 14, 38] and size of the heat exchangers

From these estimated overall heat-exchanger coefficient the area of the heat exchang-

ers is estimated by using equation 4.2 and the resulting sizes of the heat exchangers and all components are shown in table 5.4. These numbers are though rough estimate and for more detail each heat exchanger has to be designed individually to get more realistic heat exchanger surface.

5.4.2 Cost of components

Quotation from expert in the geothermal business are used to estimate the purchased equipment cost (PEC) [41]. From the PEC the total capital investment (TCI) can be estimated and the rule of thumb used that the PEC is about one third of TCI. The component size and cost is shown in table 5.5.

Component	Size	Cost 10^6 ISK	Part %
Turbine	9.5 MW	826.5	58
Pump	0.25 MW	18	1.3
Thermal oil loop	7967 m ²	462	32.4
Boiler	687 m ²	40	2.8
Condenser	990 m ²	57.5	4
Cooling system	102 m ²	6	0.4
Recuperator	250 m ²	14.5	1
Sum	-	1424.5	100

Table 5.5: Rough estimation of the purchased equipment cost (PEC) [41]

The estimated total capital investment (TCI) from the purchased equipments cost is about 4273 million ISK and has accuracy of about 50 %. The most expensive parts are the turbine and the furnace gas heat exchanger. By using equation 5.2 and 5.3 and the same assumption listed in chapter 5.3.1 the levelized cost of electric energy is estimated to be about 6.7 ISK/kWh, which is higher than estimated with the method in the preceding chapter.

The bottom up metod was also used for the steam Rankine cycle and the result were very similar to the result from the method in the preceeding chapters and therefore it is not included here.

6 Conclusion

Currently, Elkem Iceland produces two kinds of products, ferrosilicon and Microsilica, but it has all the potential to produce the third product from recovered heat. It could be electricity, steam for industrial use or water for district heating.

The focus of this study was to investigate waste heat utilization at a ferrosilicon plant at Grundartangi and use the waste heat to produce work. The main part was comparison of thermodynamic working cycles for electricity production but also measurements and data analysis to estimate the energy and exergy flows of the furnace were considered.

The production of ferrosilicon involves large exergy destruction, estimated to be 46.5 MW, and the exergetic efficiency of the furnace is about 30 %. The energy analysis shows that much of the energy used in the production of ferrosilicon at Grundartangi goes out to the environment as waste heat. Only 35.6 MW of the 98 MW of the energy supplied to the process is retrieved as chemical energy in the product.

Another result of the exergy analysis is that there is a potential to get higher grade energy from the cooling system. With the current setup the temperature increase in the cooling water of the furnace is from 40 to 50 °C and according to measurements, the heat dissipated is about 13 MW. In terms of exergy the maximum reversible work that this heat source can give is about 1 MW. A lot of exergy is destroyed by using cold cooling fluid. If heat recovery at Grundartangi is proposed, considerations should be taken to utilize this heat by changing the cooling system to increase the temperature is done in Elkem Thamshavn.

For the generating electricity, 5 setups of thermodynamic cycles where considered, two based on steam Rankine and three based on ORC with Toluene as a working

fluid. The maximum net power produced with the best configuration of a steam Rankine cycle was about 8 MW. That was achieved by utilizing heat in the furnace gas and from the cooling system. But as mentioned above the low quality of the heat from the cooling system reduces the possibilities for using the heat. Only about 330 kW are used of the total 13 MW available in the cooling system.

The best ORC configuration shows better performance than the steam Rankine cycle and has the maximum net power about 10 MW. The design utilizes both the hot furnace gas and the cooling system. The temperature range of the cooling system fits better to the ORC as a preheater before the recuperator and that leads to utilization of 940 kW of the heat, available in the cooling system.

If design changes of the cooling system are not feasible the heat can be used to produce steam or hot water for district heating. Furnace nr. 3 at Elkem Iceland can supply about 11800 m³/day of 80 °C hot water for district heating. A nearby community, Akranes, uses district heating and the maximum load in the winter time never exceeds 9000 m³/day. Therefore Elkem Iceland could supply all the hot water for Akranes today and in the near future.

A preliminary capital cost estimate was performed for the best ORC and the steam Rankine cycle configuration. The cost estimate for the steam Rankine cycle is based on power output and is about 50 % accurate and the ORC is based on quotation from a specialist on component price and has similar accuracy. The base for the economic analysis of the steam Rankine cycle is the capital cost of geothermal power plants in Iceland. The estimated total investment cost is about 2.5 billions for the steam Rankine cycle and 4.3 billions for the ORC cycle. The estimate is for the steam Rankine cycle is most likely an overestimate as concluded in chapter 5.2. The levelized cost of electrical energy produced for the steam Rankine cycle and the ORC is about 4.6 and 6.7 ISK/kWh, respectively, with an accuracy of 50 %. The reason that the ORC cycles has higher levelized cost of electrical energy is because it need more components. This cost of producing electricity is not feasible in Iceland and this kind of electricity needs to be subsidized to be profitable.

6.1 Further Studies

To get a more reliable estimate on the net power production it is important investigate the furnace gas composition. It is important to get the true minimum temperature that the furnace gas can go down to, before condensation of sulphuric acid starts to cause trouble. The minimum temperature assumed in this study was 220 °C but this limit has big influence on electricity production. Another interesting part also regarding the furnace gas is to look more closely at the boiler design with focus on

fouling and scaling.

In the optimization of the ORC configurations an interesting behavior of the pinch restriction deserves more consideration. Usually the pinch restriction are where the working fluid exits the boiler to maximize the temperature of the fluid. However in the case of the ORC the pinch is in the middle of the boiler and it is interesting to look closer at this behavior.

With regard to thermodynamic analysis, cogeneration could be investigated further. If design changes in the cooling system are not feasible, the low temperature heat source could be used as a preheater for district heating and a Rankine cycle on the top, which utilizes the high temperature heat from the furnace gas for electric production.

Another interesting perspective is to combine heat recovery at Elkem Iceland with heat recovery at an aluminum smelter which is currently operating close by. In the aluminum smelter, low temperature heat sources are available and the smelter could act as a preheater for the working fluid in a working cycle. The working fluid would then be led to the furnace at Elkem to be superheated and produce power in a turbine. This would increase the net power output, compared to the output in this study, because the lower temperature limit for the furnace gas is so high. It would be very interesting to see the results for this kind of heat recovery.

A Measurements and data analysis

A.1 Summary

The objective is to estimate the heat flow from an electric arc furnace. The furnace under consideration is furnace nr. 3 in Elkem Iceland at Grundartangi. Three heat flows will be considered: heat flow in off gas, \dot{Q}_{OG} , heat flow in cooling system, \dot{Q}_{CS} , and heat flow directly from the furnace, that is furnace sides, \dot{Q}_{FS} , and furnace bottom, \dot{Q}_{FB} . The heat flows are shown on figure A.1 which is a simplified schematic of furnace 3.

The estimated heat flows are summarized in table A.1.

	MW	%
\dot{Q}_{OG}	43.5 \pm 4	76.3
\dot{Q}_{CS}	12.7 \pm 0.9	22.3
\dot{Q}_{FB}	0.45 \pm 0.2	0.8
\dot{Q}_{FS}	0.33 \pm 0.13	0.6
Total	57 \pm 5.2	100

Table A.1: Summary of heat flows

The result in table A.1 is very close to numbers given in the literature [37]. There a typical share of loss due to off gas is 65 - 75 %, cooling water 15 - 20 % and radiation 5 - 10 %.

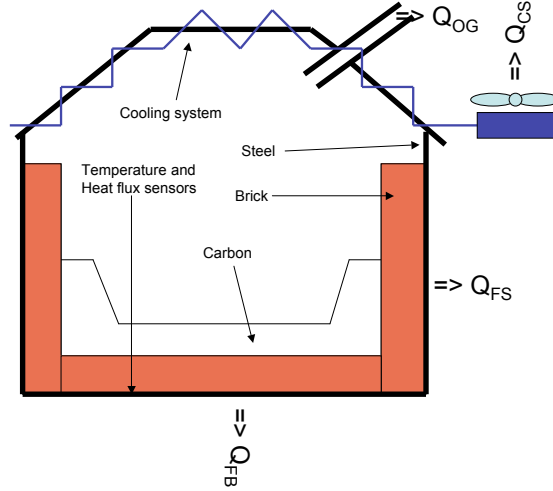


Figure A.1: Simplified schematic of furnace 3 and the heat flow under consideration

A.2 Off gas

When the gases from the crater rise up above the charge surface and are mixed with excess air they burn and release heat. The amount of excess air determines the off gas temperature. These gases then leave the furnace through off gas channels and to a heat exchanger which exchanges heat to the surrounding air. After the off gas has been cooled down the off gas is put through a filter which filters out SiO_2 or Microsilica®.

At Elkem measurements were done with pitot tubes to measure the flow. These measurements were done 9th of October, 2008 and the furnace load was 43 MW. The results are illustrated in table A.2.

Furnace Load	43 MW
Off gas flow	273 507 Nm^3/h
Off gas density	1.3 kg/Nm^3

Table A.2: Elkem pitot measurements [44]

The off gas is mostly composed of air and is therefore approximated as air and the

following equation can be used to calculate the off gas heat flow:

$$\dot{Q} = \dot{m} \cdot (h_1 - h_2) \quad (\text{A.1})$$

where \dot{Q} is the heat flow, \dot{m} is the mass flow of the offgas and the h_1 and h_2 are enthalpies before and after the heat exchanger.

The off gas is at 450 °C in the chimney and is cooled down to 216 °C in the heat exchanger. The heat load of the heat exchanger, Q_{HE} , and the total energy in the off gas, Q_{OG} , are shown in table A.3.

Q_{OG}	43.5 ± 4 MW
Q_{HE}	24 ± 2 MW

Table A.3: Heat load of heat exchanger, Q_{HE} , and total energy in off gas, Q_{OG}

A.3 Cooling system

The cooling system cools the furnace hut and the off gas channel and uses water in a closed system. After absorbing the heat the heated water goes to a heat exchanger where air is forced to flow over the pipes and cools the water. The cooling water is led to this heat exchanger in a big pipe where it is possible to measure the flow with Ultrasonic Flowmeter. If the flow and the temperature difference is known it is possible to estimate the cooling load with following equation:

$$\dot{Q} = \dot{m} \cdot c_v \cdot \Delta T \quad (\text{A.2})$$

where Q is the cooling load, \dot{m} is the mass flow in the pipe, c_v is the constant volume specific heat for water and ΔT is the temperature difference over the heat exchanger.

A.3.1 The basics

The doppler ultrasonic flowmeter used is *Polysonic Master Series Model MST-P* from Polysonic. This kind of meter uses doppler effect, that is the concept that frequency changes with motion, to measure the flow in pipes. The Ultrasonic Flowmeter sends

signal into the pipe, through transducers, with frequency around 0.6 MHz and the signal is reflected by particles, gas bubbles, flow disturbances and fluid discontinuities. Then the meter detects the changes in frequency of the signal and can then determine the flow rate.

The measured flow rate, V , is given in [m/s] and to convert it to mass flow the following equation is used:

$$\dot{m} = V \cdot \rho \cdot A = V \cdot \rho \cdot \frac{D_i^2 \cdot \pi}{4} \quad (\text{A.3})$$

where ρ is density, A is cross sectional area and D_i is inner diameter of the pipe.

A.3.2 Setup

The measurements were made 27th of November, 2008. The setup of the pipe and places where measurements were made are on figure A.2. The pipe inner diameter is $D_i = 508$ mm and it is a DIN 2458 and DIN 1628 standard.

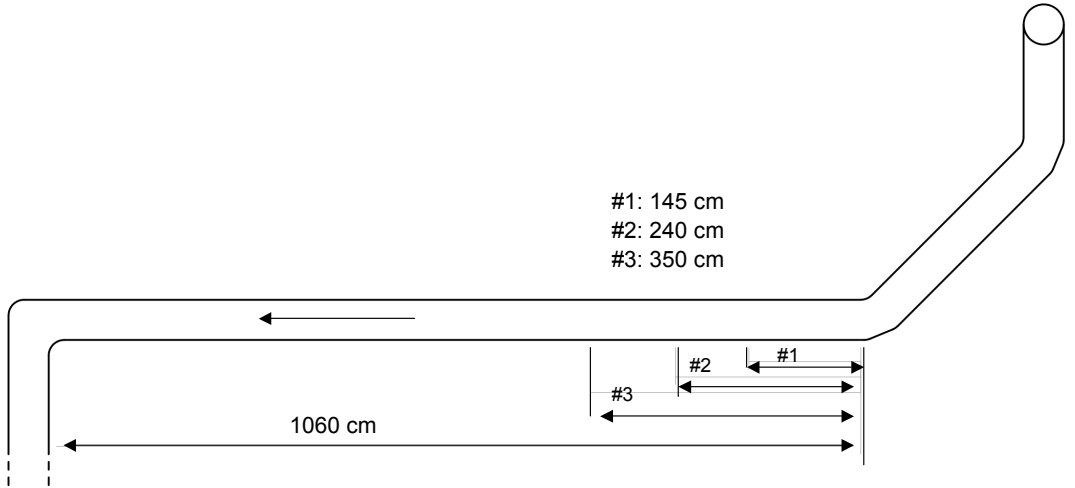


Figure A.2: The pipe and locations of measurements

Measurement were made in 3 locations as seen on figure A.2. In location 1 and 2

measurements where made in both directions. The statistic about the measurements are in table A.4. There is presented the sample size, N , the mean, \bar{v} , the standard deviation, s , the range, r , and the direction of the measurements. Direction meaning which way, up- (\rightarrow) or downstream (\leftarrow), the signal is transmitted by the transducers.

Location	N	\bar{v} [m/s]	s	r	Direction
1_a	44	2.016	0.038	0.216	\leftarrow
1_b	22	2.127	0.045	0.208	\rightarrow
2_a	78	2.001	0.042	0.200	\leftarrow
2_b	34	2.116	0.033	0.144	\rightarrow
3_a	56	2.082	0.039	0.168	\leftarrow
all	234	2.0771	0.054	0.345	both

Table A.4: The statistic about the measurements

The measurements made upstream give higher values than made downstream. According to the manual [30] the transducers will work equally well facing either direction. A notice is though given that it is good to let the transducer "look" away from potential noise sources. Therefore a noise source could have been disturbing the signal.

A boxplot of all measurement is presented in figure A.3 and it can be seen their that the measurements upstream give higher values than the those made downstream, though at the last location, location nr. 3, the values get closer to those measured upstream in the other locations.

The total mean is $\bar{v}_{tot} = 2.0771 \approx 2.1$ and the error is defined as 2 standard deviations that is $e = \pm 2 \cdot \sigma = 0.108 \approx 0.1$. The mass flow is then calculated from equation A.3:

$$\dot{m} = 2.1 \text{ [m/s]} \cdot 983 \text{ [kg/m}^3] \cdot \frac{0.508^2 \text{ [m}^2] \cdot \pi}{4} \approx 420 \text{ kg/s} \pm 20 \text{ kg/s} \quad (\text{A.4})$$

A.3.3 Temperature difference

The temperature is logged automatically by Elkem Iceland before, T_L , and after, T_H , the heat exchanger. In figure A.4 the temperature and the temperature difference, ΔT , can be seen. As illustrated on figure A.4 the load in the furnace is reduced in the beginning of this time series but is restored to normal in about 8 hours and is that part regarded as steady state conditions. Because of this load variations the

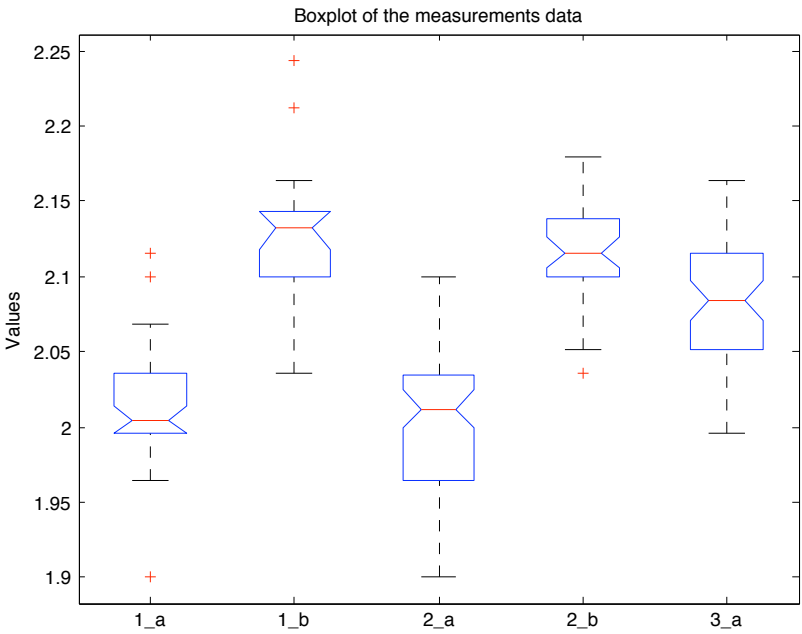


Figure A.3: Boxplot of the measurement data

unsteady part of the time series is not used.

The statistic about the temperature difference and the furnace load is listed in table A.5.

	N	\bar{x}	s	r
ΔT	91	7.50	0.54	2.8
Furnace load	100	45.14	0.72	4.29

Table A.5: The statistic for the temperature difference and furnace load

Therefore the temperature difference is:

$$\Delta T = 7.5 \text{ }^{\circ}\text{C} \pm 0.1 \text{ }^{\circ}\text{C} \tag{A.5}$$

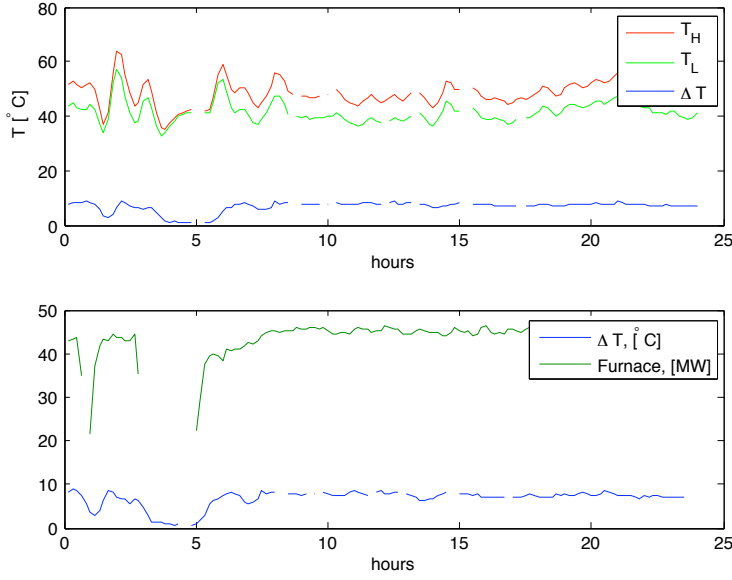


Figure A.4: Temperature measurements from 12:25 26.11 to 12:25 27.11

A.3.4 Estimated Cooling Load

The estimated cooling load is calculated from equation A.2 where $c_v = 4.03$ [kJ/kg K] at pressure 4 bar and temperature 50 °C.

$$\dot{Q}_{CS} = \dot{m} \cdot c_v \cdot \Delta T = 12.7 \text{ MW} \pm 0.9 \text{ MW} \quad (\text{A.6})$$

A.4 Directly from furnace

A.4.1 Furnace bottom

On the bottom of the furnace are 61 temperature sensors and three heat flux sensors and they are logged by Elkem Iceland. One way to estimate the total heat flow from the furnace bottom is to find the relation between the temperature and heat flux and estimate the heat flux in each point where temperature is measured. Another way

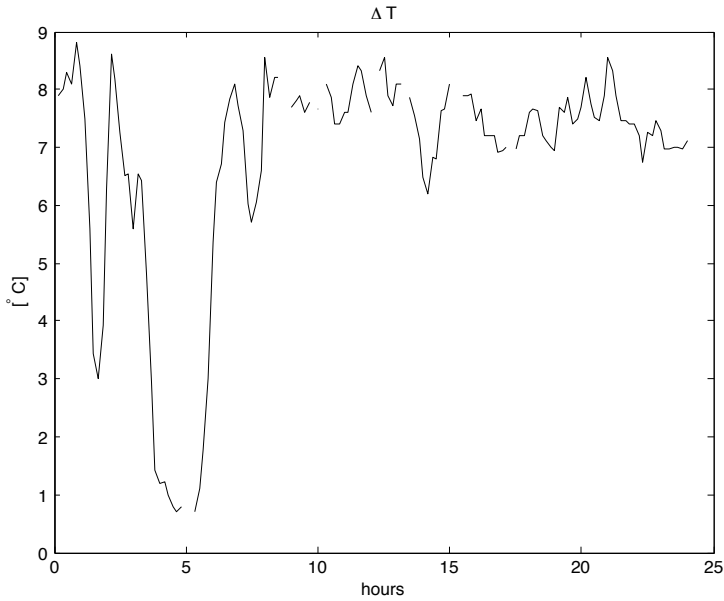


Figure A.5: The temperature difference over the heat exchanger

of estimation is to disregard the temperature measurements and take the average of the heat flux and multiply with the total area. The later is more rough estimate and is done for comparison.

Heat transfer can be in three forms conduction, convection and radiation. The molten metal in the furnace transfers heat with convection and convection to the furnace bottom. The heat transfers with convection through the bottom and the under the furnace it is transferred with forced convection because there is a fan which blows air through. The radiation isn't taken into consideration.

A.4.1.1 Sensors

In figure A.6 the arrangement of the temperature and heat flux sensor is illustrated. The sensors marked 3.3, 8.2 and 8.5 also measure heat flux.

Their placement in the cross section is illustrated in figure A.1. The time series used is from 27th of November, 2008, from 5:20 in the morning to 12:50 the same day and the time interval is 10 minutes. The mean furnace load during this period was

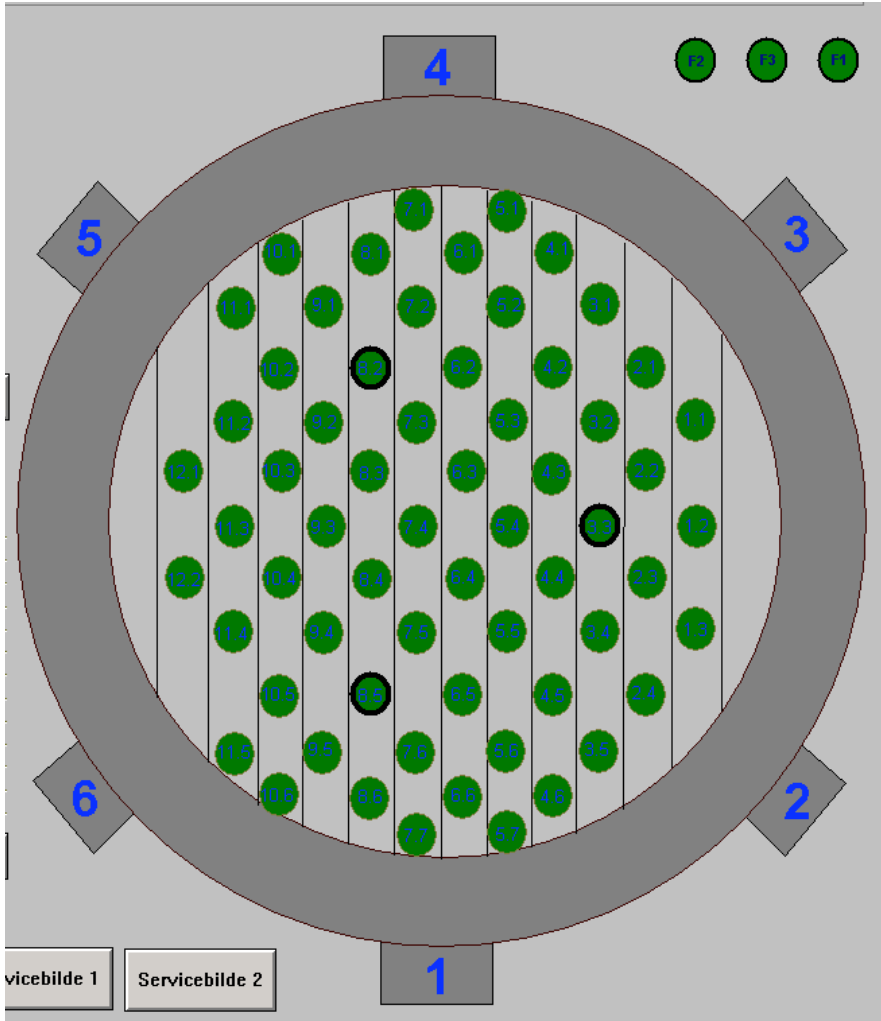


Figure A.6: The arrangement of temperature, green filled circles, and heat flux sensors, black circles

45 MW. A contour plot of the temperature distribution in the furnace bottom is illustrated in figure A.7. There it can be clearly seen the temperature is higher in the center and then cooler near the side of the furnace.

In figure A.8 the furnace load, temperature and heat flux of sensor nr. 3.3 is plotted. A scatter plot, temperature vs. heat flux, is also in figure A.8. The scatter plot shows that there is no obvious relation between the temperature and heat flux in this

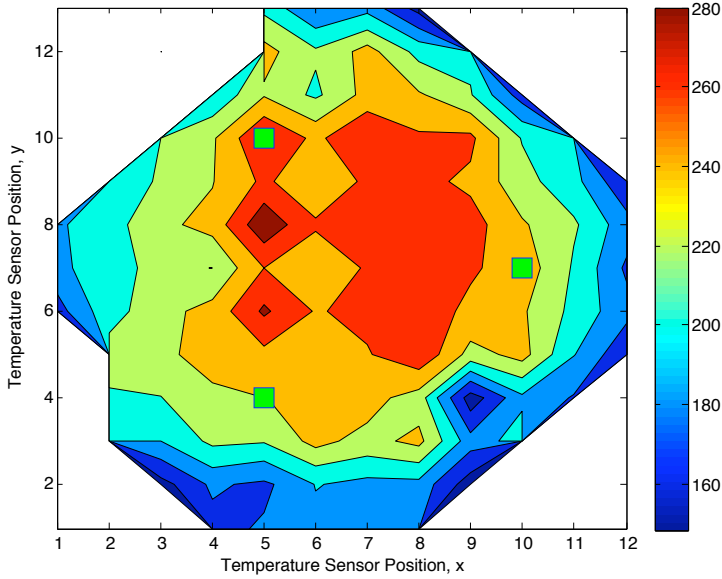


Figure A.7: Contour plot of the furnace bottom temperature at 5:20 27th of November. The green boxes are the positions of the heat flux sensors

point, because the temperature rises in these 8 hours up about 12 °C but the heat flux remains constant. This is also true for the other two heat flux sensors.

The outer diameter of the furnace is about 12.3 m. Therefor the cross sectional area of the furnace bottom is $A = \pi \cdot \frac{12.3^2}{4} = 118.8 \text{ m}^2$. The average area of each temperature sensor is $dA = \frac{78.5}{61} = 1.95 \text{ m}^2$ if assumed that the sensor are equally spaced in the furnace bottom.

A.4.1.2 The heat flow

The relation is found by using simple linear regression model. Other model considered were second-degree polynomial and exponential models but did not give good results. The simple linear regression model and the regression coefficient are

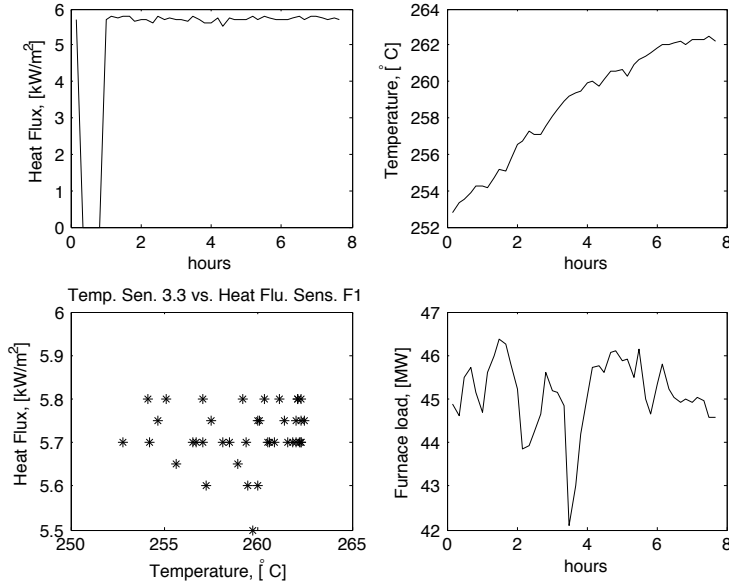


Figure A.8: Temperature and heat flux for sensor 3.3 on figure A.6

$$\hat{q} = \beta_0 + \beta_1 \cdot t \quad (\text{A.7})$$

$$\hat{q} = -6.4638 + 0.0451 \cdot t \quad (\text{A.8})$$

were \hat{q} is the heat flux, [kW/m²], and t is the temperature [°C]. The data and the model are plotted in figure A.9. The coefficient of determination for the model is $R^2 = 0.80$ which mean that this model accounts for 80 % of the variability in the data.

For each temperature sensor the heat flux, $dq_{i,j}$, is estimated by the simple linear model. A estimation of the total heat flow is then

$$\dot{Q}_{bottom,1} = dA \cdot \sum dq_{i,j} = 460 \text{ kW} \quad (\text{A.9})$$

Another way of estimation is to disregard the temperature and doing some "back of an envelope" calculations and find the mean heat flux from these three sensors, $q_m = 5.47 \text{ kW/m}^2$ and then multiply it with the total area of the furnace bottom:

$$\dot{Q}_{bottom,2} = A \cdot q_m = 650 \text{ kW} \quad (\text{A.10})$$

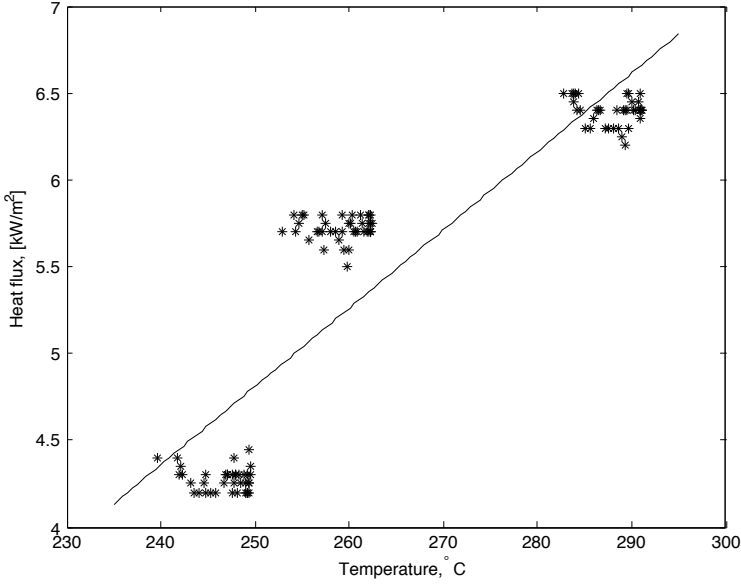


Figure A.9: The linear relation for temperature and heat flux, $R^2 = 0.80$

When comparing these two estimates, equations A.9 and A.10, we can see that the error is a big part of this number the estimated heat flow is:

$$\dot{Q}_{FB} = 450 \pm 200 \text{ kW} \quad (\text{A.11})$$

A.4.2 Furnace sides

The sides of the furnace are cooled with free convection with the surrounding air and radiation. There are no heat flux or temperature sensor in the sides of the furnace so it is quite difficult to estimate the heat flow from the sides. Thermal pictures of the furnace, e.g. in figure A.10, were used to estimate the surface temperature.

The maximum furnace temperature is about 275 °C and the average is 135 °C. These temperature are similar to the furnace bottom. The furnace is about 4 m in height and has radius about 6.3 m and therefore the total area of the furnace is about 154 m².



Figure A.10: Infrared picture of furnace 3 in Elkem Iceland

A.4.2.1 Radiation

To estimate the radiation from the sides the following relation can be used for hot convex object in large enclosure :

$$\dot{Q}_{rad} = \sigma \cdot \epsilon \cdot A \cdot (T_w - T_{\infty}) \quad (\text{A.12})$$

where σ is the Stefan-Boltzmann constant, ϵ is emissivity, A is the area and T_{∞} and T_w are the temperature of the surroundings and the object, respectively.

The furnace sides are divided in to 6 sections where the temperature is similar, listed in table A.6, and the heat flow calculated for each. The emissivity is assumed $\epsilon = 0.9$ [14] and the surrounding temperature was $T_{\infty} = 23^{\circ}\text{C}$.

The total heat flow due to radiation is therefore estimated as:

$$\dot{Q}_{rad} = 230 \pm 80 \text{ kW} \quad (\text{A.13})$$

Section	1	2	3	4	5	6
Area [%]	5	5	20	20	30	20
Ave. T_w [°C]	180	100	250	135	150	80
\dot{Q}_{rad} [kW]	13.9	4.7	108.6	32.4	29.1	40.3

Table A.6: Estimation of the radiation from the furnace

or average heat flux of $q_{rad} = 1.45 \text{ kW/m}^2$.

A.4.2.2 Convection

Convection can be calculated by following equation:

$$\dot{Q}_{conv} = h \cdot A \cdot (T_w - T_\infty) \quad (\text{A.14})$$

where h is heat-transfer coefficient. To estimate the heat-transfer coefficient, h , the surface of the furnace can be simplified as a big cylinder. It can be treated as vertical plate because $\frac{D}{L} \geq \frac{35}{Gr_L^{1/4}}$ is valid. The film temperature, T_f , is estimated on the average wall temperature of the furnace, $T_w = 135^\circ\text{C}$, and the surroundings, $T_f = \frac{T_w + T_\infty}{2}$. Based on the film temperature the properties of the air are defined. The Rayleigh number for this situation is therefore:

$$GrPr = 3.186 \cdot 10^{11} \quad (\text{A.15})$$

and the Nusselt number is then $Nu = 762$ and the estimate of the heat-transfer coefficient is:

$$h = 5.75 \text{ W/m}^2\text{K} \quad (\text{A.16})$$

The estimated heat flow because of convection is therefore:

$$\dot{Q}_{conv} = 100 \pm 50 \text{ kW} \quad (\text{A.17})$$

or the average heat flow is $q_{conv} = 0.64 \text{ kW/m}^2$.

Combined

The combined estimate of the radiation and convection is :

$$\dot{Q}_{FS} = \dot{Q}_{rad} + \dot{Q}_{conv} = 330 \pm 130 \text{ kW} \quad (\text{A.18})$$

Bibliography

- [1] MATLAB 2008a. Mathworks.
- [2] Adrian Bejan, George Tsatsaronis, and Michael Moran. *Thermal Design and Optimization*. John Wiley & Sons, INC., 1996.
- [3] S. Bramfoot, J. Dixon, J. R. Martin, and R. A. Page. The feasibility of using waste heat boilers to recover energy from the exhaust gases of electric arc furnaces. *Heat Recovery Systems*, 5(4):353 – 364, 1985.
- [4] Ünal Çamdali and Murat Tunç. Exergy analysis and efficiency in an industrial ac electric arc furnace. *Applied Thermal Engineering*, 23(17):2255 – 2267, 2003.
- [5] Vincent Cavaseno. *Process Heat Exchanges*. McGraw-Hill, 1979.
- [6] Yunus A. Cengel and Michael A. Boles. *Thermodynamics - An Engineering Approach*. Mechanical Engineering. McGraw-Hill, fifth edition edition, 2006.
- [7] M. W. Chase, C. A. Davies, J. R. Downey, D. J. Frurip, R. A. Macdonald, and A. N. Syverud. *JANAF Thermodynamic Table*, volume 14. American Chemical Society and the American Institute of Physics for the National Bureau of Standards, third edition edition, 1985.
- [8] Ulli Drescher and Dieter Bruggemann. Fluid selection for the organic rankine cycle (orc) in biomass power and heat plants. *Applied Thermal Engineering*, 27(1):223 – 228, 2007.
- [9] Íslenska Járnblendifélagid ehf. Skýrsla um grænt bókhald 2007. Technical report, 2007.
- [10] Sigurgeir Björn Geirsson. Personal communications. Orkuveita Reykjavíkur, March 2009.
- [11] Hagstofan. <http://www.hagstofan.is>, March 2009.
- [12] William Harvey. Personal communications. University of Reykjavík, February 2009.

- [13] Eiríkur Hjálmarsson. Personal communications. Orkuveita Reykjavíkur, March 2009.
- [14] J. P. Holman. *Heat Transfer*. McGraw-Hill Higher Education. Elizabeth A. Jones, ninth edition edition, 2002.
- [15] Tzu-Chen Hung. Waste heat recovery of organic rankine cycle using dry fluids. *Energy Conversion and Management*, 42(5):539 – 553, 2001.
- [16] Barry Hyman. *Fundamentals of Engineering Design*. Prentice Hall, second edition, 2003.
- [17] Íslenska Járblendifélagid. <http://www.jarblendi.is>, January 2008.
- [18] Skúli Jóhannsson. Personal communications. Kaldara ehf., February 2009.
- [19] Stein Tore Johansen, Halvard Tveit, Sven Gradahl, Aasgeir Valderhaug, and Jon Age Byberg. Environmental aspects of ferro-silicon furnace operation - an investigation of waste gas dynamics. In *INFACON 8*, Junu 1998.
- [20] Sotirios Karellas and Andreas Schuster. Supercritical fluid parameters in organic rankine cycle applications. *International Journal of Thermodynamics*, 11(3):101 – 108, 2008.
- [21] Tadeusz Jozef Kotas. *The Exergy Method Thermal Plant Analysis*. Butterworths, 1985.
- [22] Landsvirkjun. <http://www.lv.is>, March 2009.
- [23] J. Larjola. Electricity from industrial waste heat using high-speed organic rankine cycle (orc). *International Journal of Production Economics*", 41(1-3):227 – 235, 1995. Proceedings of the 12th International Conference on Production Research.
- [24] Bo-Tau Liu, Kuo-Hsiang Chien, and Chi-Chuan Wang. Effect of working fluids on organic rankine cycle for waste heat recovery. *Energy*, 29(8):1207 – 1217, 2004.
- [25] Helge Fardal Midtdal. Effekt- og materialflyt i smelteprosess. Elkem Report, April 2007.
- [26] Erling Næss. Personal communications., June 2008.
- [27] Orkustofnun. <http://www.os.is>, March 2009.
- [28] Halldór Pálsson. Utilization of geothermal energy for power production. Lecture Notes - University of Iceland, 2007.
- [29] Robert H. Perry. *Perry's Chemical Engineers' Handbook*. McGraw-Hill, seventh edition, 1997.

- [30] Polysonic INC. *MODEL MST-P OPERATORS MANUAL*, 1989.
- [31] Mineral Resource Program. <http://minerals.usgs.gov/>, February 2009.
- [32] REFPROP. *Version 8.0, NIST Standard Reference Database 23*. the US Secretary of Commerce, 2007.
- [33] Orkuveita Reykjavíkur. <http://www.or.is>, February 2009.
- [34] Thomas Philip Runarsson and Xin Yao. Stochastic ranking for constrained evolutionary optimization. *IEEE Transacion on Evolutionary Computation*, 4(3):284–294, September 2000.
- [35] Anders Schei, Johan Kr. Tuset, and Halvard Tveit. *Production of High Silicon Alloys*. TAPIR forlag, 1998.
- [36] Hannes Frímánn Sigurðsson. Personal communications. Orkuveita Reykjavíkur, January 2009.
- [37] SINTEF Material Technology, Elkem, Tinfos, Ila and Lilleby. *Energy Recovery in the Norwegian Ferro Alloy Industry*, Trondheim, Norway, June 1995. FFF.
- [38] Engineering Toolbox. <http://www.engineeringtoolbox.com>, February 2009.
- [39] Halvard Tveit. Personal communications., June 2008.
- [40] Torbjörn Tveitan. Personal communications., June 2008.
- [41] Páll Valdimarsson. Personal communications. University of Iceland, March 2009.
- [42] Donghong Wei, Xuesheng Lu, Zhen Lu, and Jianming Gu. Performance analysis and optimization of organic rankine cycle (orc) for waste heat recovery. *Energy Conversion and Management*, 48(4):1113 – 1119, 2007.
- [43] Helgi Þór Ingason. *Athuganir á ofnstýrikerfi í kísiljárnframleiðslu*. Master’s thesis, University of Iceland, 1991.
- [44] Þorsteinn Hannesson. Personal communications. Elkem Iceland, 2008 - 2009.